

RESEARCH ARTICLE

Fire, CO₂, and climate effects on modeled vegetation and carbon dynamics in western Oregon and Washington

Tim Sheehan^{1,2*}, Dominique Bachelet³, Ken Ferschweiler¹

1 Conservation Biology Institute, Corvallis, Oregon, United States of America, **2** Graduate School, Oregon State University, Corvallis, Oregon, United States of America, **3** Department of Biological and Ecological Engineering, Oregon State University, Corvallis, Oregon, United States of America

✉ Current address: Conservation Biology Institute, Corvallis, Oregon, United States of America
* tim@consbio.org



OPEN ACCESS

Citation: Sheehan T, Bachelet D, Ferschweiler K (2019) Fire, CO₂, and climate effects on modeled vegetation and carbon dynamics in western Oregon and Washington. PLoS ONE 14(1): e0210989. <https://doi.org/10.1371/journal.pone.0210989>

Editor: Debjani Sihi, Oak Ridge National Laboratory, UNITED STATES

Received: October 7, 2018

Accepted: January 4, 2019

Published: January 25, 2019

Copyright: © 2019 Sheehan et al. This is an open access article distributed under the terms of the [Creative Commons Attribution License](https://creativecommons.org/licenses/by/4.0/), which permits unrestricted use, distribution, and reproduction in any medium, provided the original author and source are credited.

Data Availability Statement: Data produced by the MC2 model and underlying all results in this study are available in Data Basin through the url: <https://databasin.org/galleries/7fae7ecca8fe4ac0abbd84f15c1e90c4>.

Funding: This work was supported by (DB) U.S. Department of the Interior via the Northwest Climate Science Center through agreement #G12AC20495 within the framework of the research project entitled “Integrated Scenarios of climate, hydrology and vegetation for the

Abstract

To develop effective long-term strategies, natural resource managers need to account for the projected effects of climate change as well as the uncertainty inherent in those projections. Vegetation models are one important source of projected climate effects. We explore results and associated uncertainties from the MC2 Dynamic Global Vegetation Model for the Pacific Northwest west of the Cascade crest. We compare model results for vegetation cover and carbon dynamics over the period 1895–2100 assuming: 1) unlimited wildfire ignitions versus stochastic ignitions, 2) no fire, and 3) a moderate CO₂ fertilization effect versus no CO₂ fertilization effect. Carbon stocks decline in all scenarios, except without fire and with a moderate CO₂ fertilization effect. The greatest carbon stock loss, approximately 23% of historical levels, occurs with unlimited ignitions and no CO₂ fertilization effect. With stochastic ignitions and a CO₂ fertilization effect, carbon stocks are more stable than with unlimited ignitions. For all scenarios, the dominant vegetation type shifts from pure conifer to mixed forest, indicating that vegetation cover change is driven solely by climate and that significant mortality and vegetation shifts are likely through the 21st century regardless of fire regime changes.

Introduction

Expected ecosystem responses to climate change include altered fire regimes (e.g. [1–3]), insect outbreaks (e.g. [4]), hydrologic changes (e.g. [5]), altered nutrient cycling (e.g. [6]), species range shifts (e.g. [7–9]), and novel species assemblages (e.g. [10–11]). Vegetation models have been used to simulate such changes and provide resource managers projections to help their decision process [12]. Estimating associated uncertainty allows managers to modulate their strategies [12].

Dynamic Global Vegetation Models (DGVMs) are process-based models that simulate vegetation, carbon, nutrient, and hydrological dynamics. They are driven by historical climate data and climate projections from General Circulation Models (GCMs; e.g. [13]) or Earth System Models (ESMs; [14]). Sources of uncertainty in DGVM projections come from both

Northwest", P. Mote (Oregon State University) principal investigator. This organization is now called the Northwest Climate Adaptation Science Center, <https://nwcasc.uw.edu/>. The funders had no role in study design, data collection and analysis, decision to publish, or preparation of the manuscript.

Competing interests: The authors have declared that no competing interests exist.

external drivers such as climate and soil characteristics, and internal characteristics such as model structure, empirical parameter values, built-in thresholds, and inherent assumptions and simplifications.

Another source of uncertainty is the complex relationship between fire and vegetation, which takes place over a range of spatial and temporal scales [15]. Shifts in fire regime cause vegetation-altering feedbacks (e.g. [16–17]). The type and level of complexity of fire models adequate for management-relevant vegetation modeling remains unclear [18]. Researchers have implemented a variety of models [19–21] which may or may not include fuel types, fuel moisture, ignitions sources, fire suppression, rate of spread, and energy release component calculation [18, 22]. Disturbance modeling at the landscape scale is discussed in [23], and fire model limitations and uncertainties in global vegetation models are described in [18, 22]. While comparing results among DGVMs using different fire models provides one way to characterize uncertainty, modifying the assumptions within a single DGVM's fire model is another method for sensitivity analysis and the exploration of fire-related uncertainty.

An additional source of uncertainty is the assumptions of CO₂ effects on plant productivity. CO₂ concentration effects on the water use efficiency and productivity of many species is not well known (e.g. [24]). Increased productivity has been attributed to the CO₂ fertilization effect, but plant responses at large scales, with complex species assemblages, and combined with concurrent warming are uncertain [25]. Free-air CO₂ enrichment experimental results (FACE) [26] have shown that increased CO₂ can cause an increase in water use efficiency (WUE), leaf area index (LAI) and net primary productivity (NPP), but other factors, such as nutrient availability, may constrain responses over time (e.g. [27]). Species-specific response can modulate plant responses (e.g. [27–28]) and increased NPP may not increase C stocks [24] just as increased WUE may not always lead to increased growth [29]. Uncertainties in the CO₂ fertilization effect underscore the importance of testing different assumptions with DGVMs to explore vegetation response.

A previous study simulated climate change effects on fire and vegetation in the Pacific Northwest using the MC2 DGVM [1]. That study characterized the uncertainty due to different atmospheric CO₂ concentrations, climate drivers, and anthropogenic fire suppression actions. Fire occurrence and effects were driven by fuel condition thresholds and unlimited ignition sources. That study used a modest CO₂ fertilization effect proportional to atmospheric CO₂ concentration.

In this study, we evaluate uncertainty due to model assumptions regarding fire occurrence and CO₂-driven WUE. We compare results from unlimited ignitions and fixed fuel thresholds to those with stochastic ignition occurrence and ignition propagation based on fuel conditions. We also compare results obtained with and without CO₂ fertilization effect. We address the following research questions concerning vegetation and carbon dynamics in the MC2 DGVM:

1. What are the consequences of model assumptions about wildfire ignitions on spatial and temporal fire effects, carbon dynamics, and vegetation dynamics?
2. What are the consequences of model assumptions about CO₂ fertilization effects on carbon and vegetation dynamics?

Methods

Study area

The study area (Fig 1) consists of portions of Oregon and Washington west of the Cascade Mountain Range crest that include Coast Range, Klamath Mountains/California High North Coast

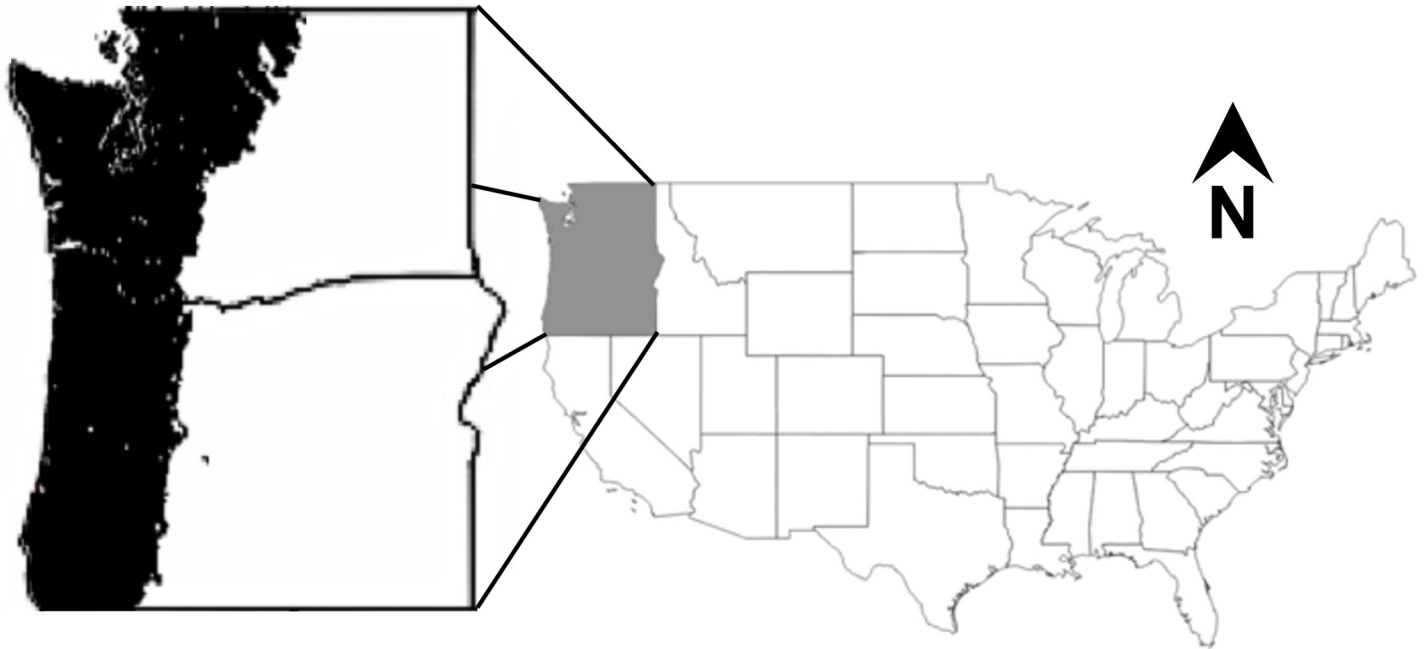


Fig 1. Study area. Portions of Oregon and Washington west of the Cascade Mountain Range crest.

<https://doi.org/10.1371/journal.pone.0210989.g001>

Range, Willamette Valley, Puget Lowlands, Cascades, and North Cascades Level III Ecoregions [30]. This area falls under strong coastal influence with mild, wet winters and dry summers.

Model description

We used the MC2 dynamic global vegetation model (DGVM) [31] to simulate potential vegetation shifts, carbon fluxes, and wildfires. We simulated potential vegetation without land use effects, and with previously defined model parameterization and protocol for the conterminous United States (detailed in [31]).

MC2 does not simulate species, but instead simulates combinations of life forms in functional vegetation types. Woody lifeforms (trees and shrubs) are distinguished by leaf phenology (evergreen vs. deciduous) and morphology (needleleaf vs. broadleaf). The woody lifeforms and the relative dominance of C3 versus C4 grasses (including sedges and forbs) are simulated using climate thresholds. Carbon thresholds are used to distinguish broad vegetation types ranging from forest to grassland.

The fire module simulates fire occurrence and fire effects including area burned, mortality, consumption of aboveground biomass, carbon emissions, and nitrogen volatilization. Fire occurrence is simulated as a discrete event. The module runs on a pseudo-daily time step and derives a randomly distributed set of daily precipitation amounts from monthly precipitation values. Fuel types are derived from carbon stocks, and their characteristics are determined by weather effects on their moisture content (see [1] for a detailed description). Per vegetation type fire return intervals (FRIs) and time since last fire are used to limit the maximum portion of a grid cell burned. Fire occurrence is based on fuel condition thresholds and assumed unlimited ignitions. Fire suppression is simulated by assuming fires below empirical fuel condition thresholds can be extinguished while those above cannot.

For this study, we added an optional, three-stage stochastic ignition algorithm to MC2. Stage one uses a per-day ignition source probability and a Monte Carlo draw to determine

whether a grid cell is exposed to an ignition source. Stage two checks fuel conditions for fine fuels moisture code (FFMC) [32] and buildup index (BUI) [33]. With unlimited ignitions, both FFMC and BUI must exceed a cell's vegetation type's threshold for a fire to be simulated. With the stochastic algorithm, they must both exceed a specified fraction of their respective thresholds. The third stage uses a Monte Carlo method to determine whether or not an ignition source initiates a fire. The probability of fire initiation is determined using the Chapman-Richards function:

$$s = (1 - e^{(-k*ffmc_thresh_frac)})^2 \tag{1}$$

where *ffmc_thresh_frac* is defined as the fraction of the FFMC threshold, adjusted to offset the curve so that values below the minimum threshold produce an initiation probability of zero, and values near the maximum threshold produce a initiation probability near 1.0. It is calculated as:

$$ffmc_thresh_frac = \max((ffmc_min_frac - ffmc_max_frac), 0) \tag{2}$$

k in (2) is the Chapman-Richards constant and is calculated as:

$$k = \frac{-\ln(1 - \sqrt{0.99})}{ffmc_max_frac - ffmc_min_frac} \tag{3}$$

where *ffmc_min_frac* is the fraction of the FFMC threshold below which fire initiation approaches 0, and *ffmc_max_frac* is the fraction of the FFMC threshold where it approaches 1.

For this study, the daily ignition source probability was 0.001, the *threshold_fraction* was 0.6 and *ffmc_min_frac* and *ffmc_max_frac* were 0.6 and 0.99 respectively (Fig 2).

To implement the CO₂ fertilization effect on WUE, MC2 uses a multiplier applied directly to production and transpiration. It is calculated as:

$$multiplier = 1 + (effect_param - 1) * \log_2 \frac{current_co2_conc}{baseline_co2_conc} \tag{4}$$

where *multiplier* is the value used to modify production, *effect_param* specifies the degree of the effect, *current_co2_conc* is the CO₂ concentration for the current model year, and *baseline_co2_conc* is the CO₂ concentration at which the multiplier is equal to 1.0 (350 ppm in this study). CO₂ concentrations above 350 ppm yield a positive effect and values below 350 yield a negative effect. The default CO₂ fertilization effect used in this study is 1.25 (Fig 3).

Model runs

We ran MC2 on a 1/24 degree (~4 km) grid using PRISM [34] data for the historical period (1895–2010) and CCSM4 (National Center for Atmospheric Research) climate projections for 2011–2100 downscaled using the MACA [35] algorithm which performs well in capturing fire danger indices across the western US. We used the CO₂ concentrations associated with RCP 8.5 (“business as usual”). We used the same CMIP5 climate, CO₂ projections, and soil data as in [1].

Run protocol

For this study, we ran the model with different combinations of fire and CO₂ fertilization effects (Table 1). To run without the CO₂ fertilization effect, atmospheric CO₂ concentration was held at its preindustrial value.

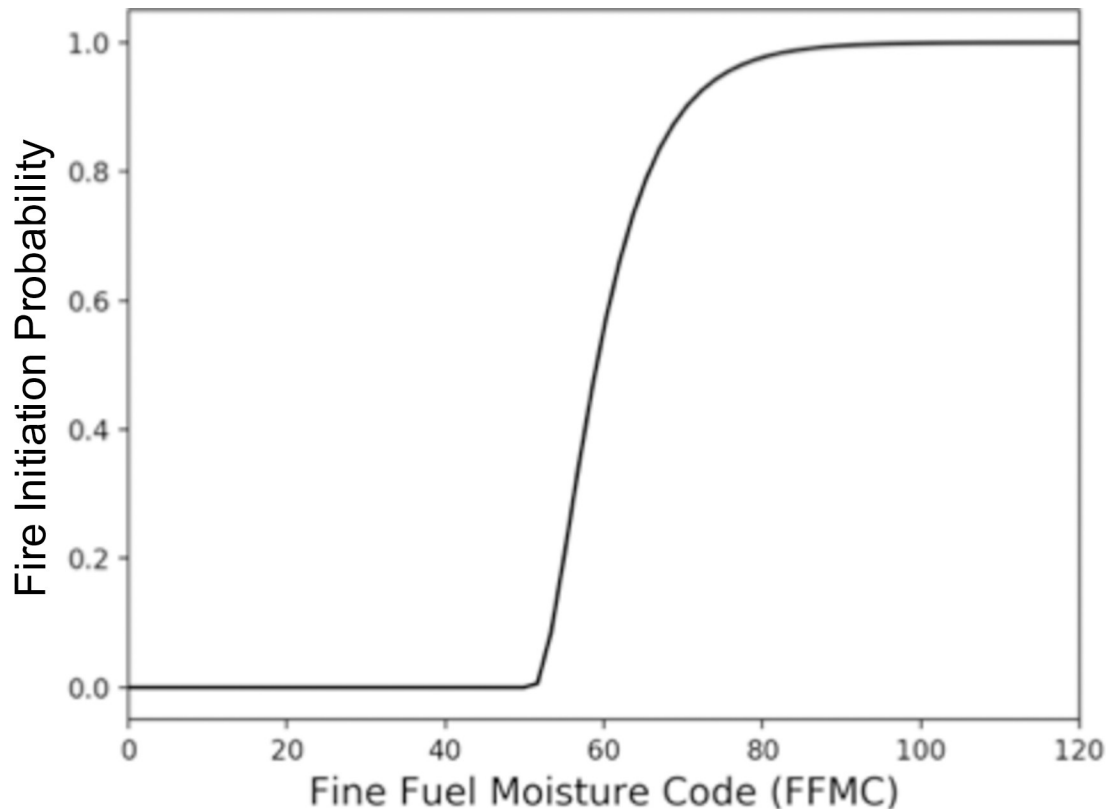


Fig 2. Example fire initiation probability curve. This example is for a vegetation type with a fine fuel moisture code (FFMC) threshold of 86, an FFMC and buildup index (BUI) minimum threshold fraction of 0.6 and an FFMC maximum threshold fraction of 1.0.

<https://doi.org/10.1371/journal.pone.0210989.g002>

Validation and comparison with other studies

For the FF-WCE and SF-WCE scenarios, we compared simulated results with the observed area burned from the Monitoring Trends in Burn Severity (MTBS) [36] fire perimeter dataset (<https://www.mtbs.gov/>) dataset. We also compared simulated results for aboveground live woody biomass (AGB), aboveground dead woody carbon (AGD), and total aboveground woody carbon (AGT) densities and pools with published modeled results based on observed Forest Inventory and Analysis (FIA) National Program (<https://www.fia.fs.fed.us/>) data ([37], hereafter, Hudiburg, available on Data Basin, <http://bit.ly/2CcZ7wK>; [38,14,39]). To reflect the influence of land use, we limited our results to non human-affected (NHA) based on the Land-Fire US 140 EVT dataset (landfire.gov; 30m x 30m).

In the Hudiburg datasets, we set densities of carbon in human-affected (HA) cells to 0 before resampling to the 1/24 degree grid used in our simulation. We adjusted carbon densities from our simulation results by multiplying the results by the ratio of NHA area to the total grid cell area. We similarly adjusted results for validation against the MTBS [36] dataset.

Analyses

We compared fire results, carbon dynamics, and vegetation change among modeled scenarios. For fire, we compared three results: 1) area with fire (AWF)—the total area of grid cells burned; 2) fraction area burned (FAB)—fraction of area burned in grid cells with fire; and 3) total area burned (TAB), the sum of (AWF * FAB) over all grid cells.

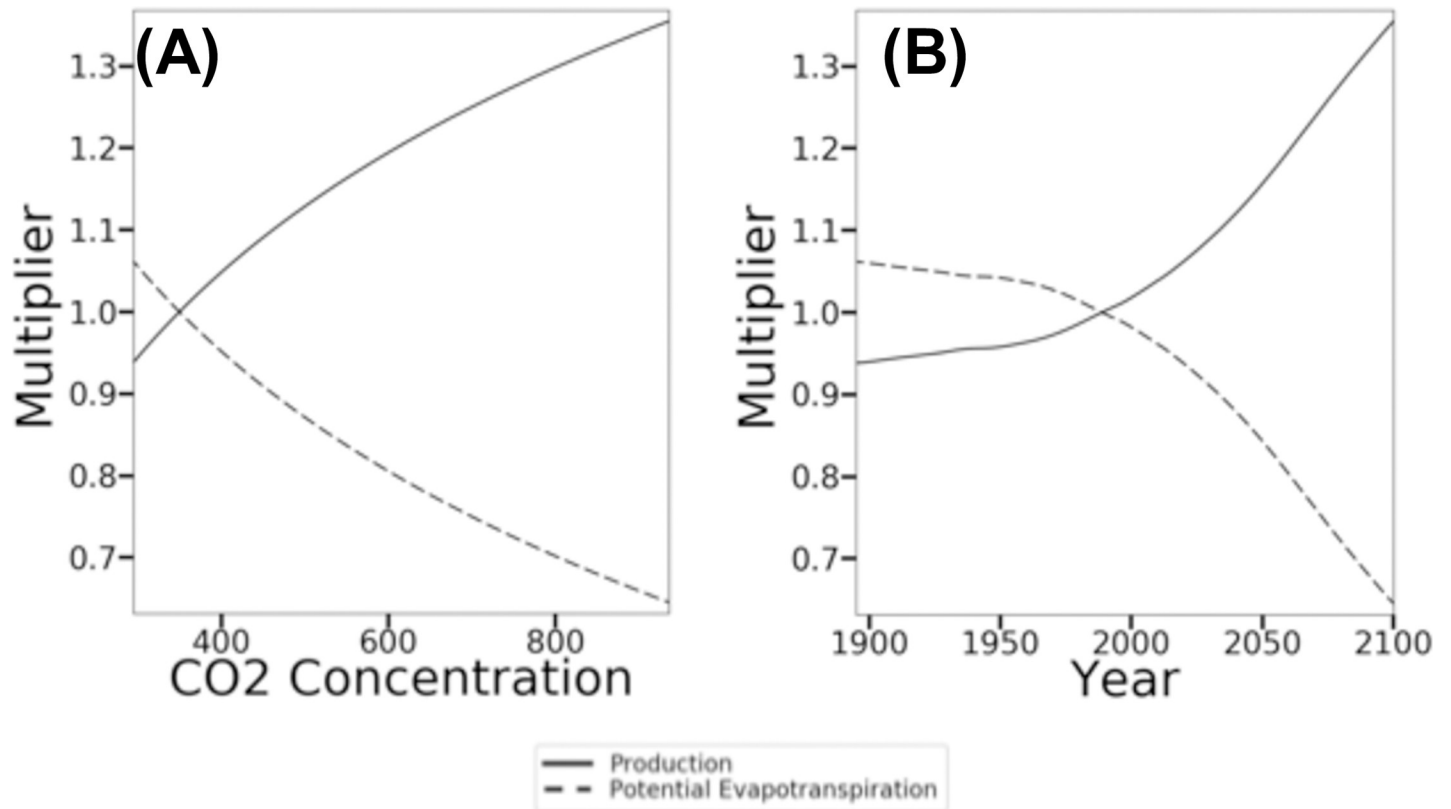


Fig 3. CO₂ fertilization effect scalar. The scalar used in MC2 to calculate production and potential evapotranspiration vs (A) atmospheric CO₂ concentration and (B) year.

<https://doi.org/10.1371/journal.pone.0210989.g003>

For carbon, we compared live and dead carbon (C) pools, total ecosystem C stocks, net primary production (NPP), net ecosystem production (NEP), net biome production (NBP), and C consumed and emitted by fire (consumed C). Results for C pools and fluxes were summarized by taking mean values over the study area for five 30-year periods: early 20th c. (1895–1924), mid 20th c. (1936–1965), late 20th c. (1971–2000), mid 21st c. (2036–2065), and late 21st c. (2071–2100).

To more easily compare vegetation cover, we reclassified vegetation types into four categories: conifer forest; temperate mixed conifer/broadleaf forest; subtropical mixed conifer/broadleaf forest; and other which includes vegetation types dominated by grasses, forbs, and shrubs (S1 Table). We then calculated the mode of the vegetation category for each grid cell for each time period and calculated the area-weighted distribution for each category.

Table 1. Fire and CO₂ fertilization scenarios used for this study’s MC2 runs.

	With CO ₂ fertilization effect (WCE for with CO ₂ fertilization effect)	Without CO ₂ fertilization effect (NCE for no CO ₂ fertilization effect)
Assumed ignitions, without fire suppression (FF for full fire)	FF-WCE	FF-NCE
Assumed ignitions with fire suppression (FS)	FS-WCE	Not modeled
Stochastic fire (SF)	SF-WCE	Not modeled
No fire (NF)	NF-WCE	NF-NCE

<https://doi.org/10.1371/journal.pone.0210989.t001>

Background climate description

Climate projections used for the future period (2011–2100) are overall hotter with decreasing summer precipitation towards the late 21st c. and increasing PET. Maximum annual and April–September average temperatures are relatively constant over the 20th c. (S1A Fig, S2 Table), with 30-year means varying by 0.2°C or less. During the 21st c. temperatures increase sharply with maximum annual temperatures 4.4°C higher, and April–September average temperatures 4.8°C higher than during the late 20th c. Annual precipitation increases by 4% from the early to late 20th c. and an additional 6% from the late 20th c. to the late 21st c. (S1B Fig, S2 Table). April–September precipitation increases 6% over the 20th c. but compared to the late 20th c., decreases by 15% during the mid 21st c. and again during the late 21st c. (S1B Fig, S2 Table). PET (calculated by MC2) increases by 3% from the early to the late 20th c., increases by 29% from the late 20th c. to the mid 21st c. and by 52% from the early 20th c. to the late 21st c. (S1C Fig, S2 Table).

Results

Validation and comparison with other studies

For simulations with fire, TAB (total area burned) is 2.3 to 2.8 times observed (Table 2). Burned areas for both observed and FF-WCE are concentrated across the southeastern corner of the study area, the central east edge, and the northeastern corner (Fig 4B and 4C). However, for FF-WCE, fire is simulated in the northernmost central portion of the area (northern Cascades) where it is not observed, and in the southeast fire is less concentrated than observed. For SF-WCE, fire occurrence is also concentrated in the southeastern and northeast (Fig 4D), but also occurs more frequently throughout non-human-influenced areas than either for observed or FF-WCE, most commonly in the Cascade Mountains, southern Coast Range, and Puget Trough (Fig 4B–4D).

Our simulated AGB ranges from 11 to 57% higher than that modeled by Hudiburg (Table 3). AGD carbon also ranges from 79 to 105% higher, and AGT carbon ranges from 28 to 68% higher. Among our simulations, AGB, AGD, and AGT are highest for NF-WCE, and lowest for SF-WCE (Table 3). AGB, AGD, and AGT densities are generally higher and more flatly distributed than Hudiburg’s (Fig 5). AGB, AGD, and AGT density distributions are flat-test for SF-WCE.

Our simulated AGB and AGT values fall below Hudiburg’s mean trend maxima for those ecoregions in our study area (Coast Range, West Cascades, and Klamath mountains; Table 3). Our simulated AGD values fall between Hudiburg’s lowest and highest mean trend maxima and below their largest mean trend maxima (Table 3).

Table 2. Area burned over the period 1985–2012 for MTBS and TAB (total area burned, AWF (area with fire) * FAB (fraction burned)) for with-fire simulations.

Scenario	Area Burned (km ²)
MTBS (km ²)	10,753
FF-WCE (km ²)	28,205
FS-WCE (km ²)	24,828
SF-WCE (km ²)	24,603
FF-NCE (km ²)	29,211

(FF-WCE: full fire, with CO₂ fertilization effect; FS-WCE: with fire suppression, with CO₂ fertilization effect; SF-WCE: with stochastic ignitions, with CO₂ fertilization effect; and FF-NCE: full fire, with no fertilization effect)

<https://doi.org/10.1371/journal.pone.0210989.t002>

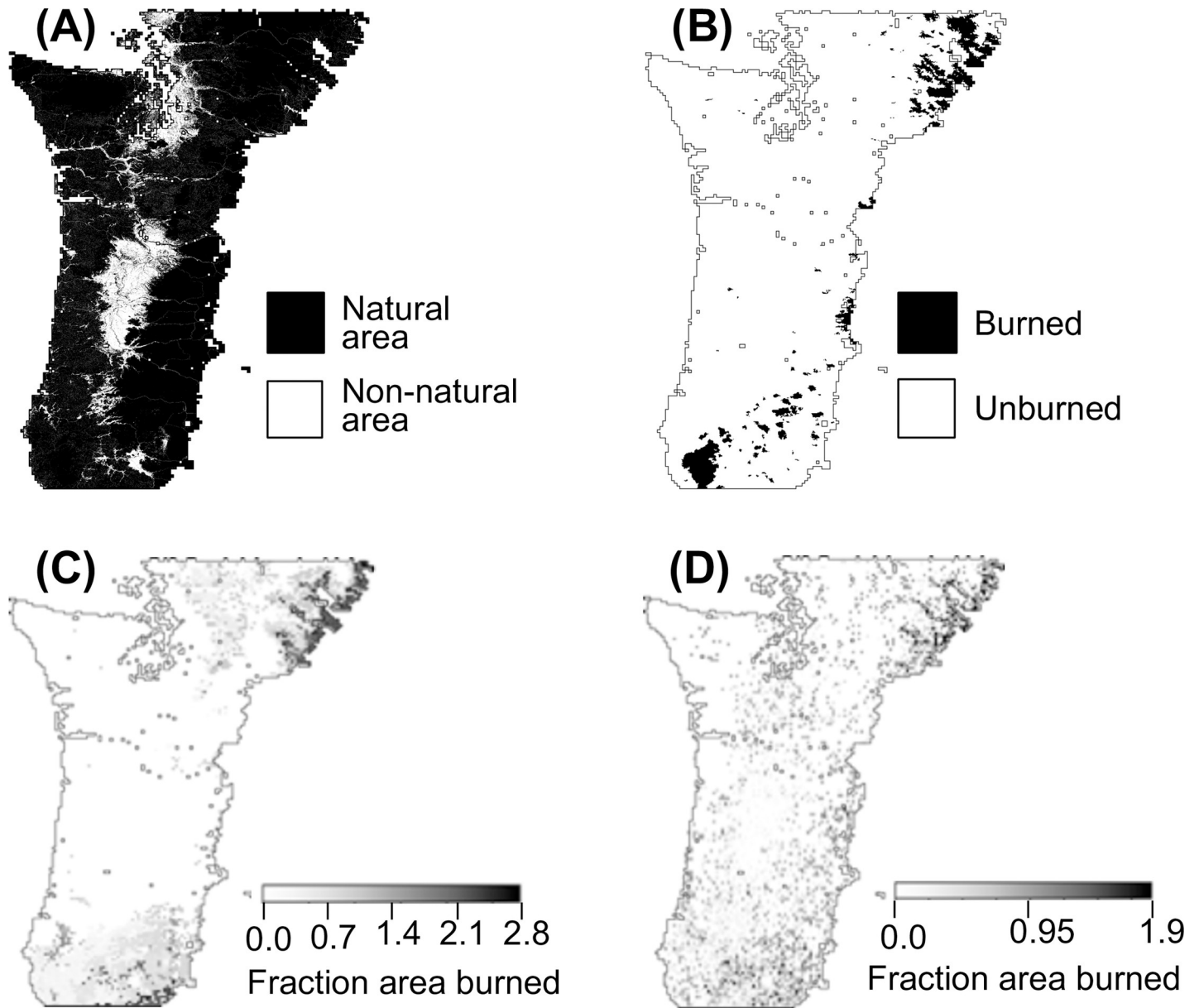


Fig 4. Measures of fire on the landscape. (A) Natural and human-affected areas as determined by reclassifying LandFire vegetation classes; (B) MTBS fire perimeters for 1985–2015; (C) Total NHA (non-human affected) area burned over 1985–2015 (sum of FAB weighted by grid cells’ NHA fraction over 1985–2015) for FF-WCE (full fire, with CO₂ fertilization effect); and (D) Total NHA area burned over 1985–2015 for SF-WCE (no fire suppression, with CO₂ fertilization effect).

<https://doi.org/10.1371/journal.pone.0210989.g004>

Our simulated AGT carbon density (Fig 6C–6E) is lowest in highly human affected (HA) areas (Fig 6A) such as in the Willamette Valley and surrounding Puget Sound. In these areas, there is little difference among values for our simulations or between our simulations and Hudiburg’s (Fig 6B).

For NF-WCE (Fig 6C) our simulated AGT carbon density is higher than Hudiburg’s over most of the study area. For FF-WCE (Fig 6D) our simulated AGT carbon density is generally lower in areas that have experienced fire and higher in areas that have not. Similarly, for SF-WCE, our simulated carbon density is lower in areas having experienced fire, but those areas are greater due to the spatially broader simulated fire occurrence (Fig 6D).

Table 3. Carbon values for Hudiburg and MC2 results.

Veg. Type	AGB Total (Pg)	AGD Total (Pg)	AGT Total (Pg)	AGB Density (gCm ⁻²) (maximum)	AGD Density (gCm ⁻²) (maximum)	AGT Density (gCm ⁻²) (maximum)
Hudiburg	1.84	0.58	2.42	26900–44200 (~50000–~70000)	2600–9500 (~8000–~1700)	38100–46800 (~58000–~84000)
FF-WCE	2.31	1.11	3.43	14205	6826	21092
FS-WCE	2.32	1.12	3.44	14266	6887	21154
SF-WCE	2.05	1.04	3.09	12606	6395	19001
NF-WCE	2.89	1.19	4.07	17772	7318	25028
FF-NCE	2.26	1.09	3.35	13897	6703	20600
NF-NCE	2.82	1.17	3.99	17341	7195	24536

NHA (non-human affected) AGB (above ground live woody biomass), AGD (above ground dead woody carbon), and AGT (above ground total woody carbon). (For Hudiburg values, absolute values were calculated from Oregon and Washington maps published in Data Basin (<http://bit.ly/2CcZ7wK>), density values are maxima of mean trends (maxima of maximum trends in parentheses) from [37] for ecoregions included in the current study; FF-WCE: full fire, with CO₂ fertilization effect; FS-WCE: with fire suppression, with CO₂ fertilization effect; SF-WCE: with stochastic ignitions, with CO₂ fertilization effect; NF-WCE: no fire, with CO₂ fertilization effect; FF-NCE: full fire, with no fertilization effect; and NF-NCE: no fire, with no CO₂ fertilization effect)

<https://doi.org/10.1371/journal.pone.0210989.t003>

Compared to other studies [38, 14, 39] in the same region, our values for NPP, NEP, and NBP are generally lower, while our values for carbon stocks are higher (Table 4).

Fire

AWF is identical for FF-NCE and FF-WCE throughout the simulation (Fig 7A, Table 5). FAB for FF-NCE is very similar to that for FF-WCE during the early 20th c. but is higher through the rest of the simulation with a peak difference of 1.08% of cell area during the late 21st c. (Fig 7B, Table 5). TAB for FF-NCE is similar to that for FF-WCE through the 20th c., but is higher during the 21st c. with a maximum difference of 0.28% during the late 21st c. (Fig 7C, Table 5).

AWF for FS-WCE is virtually identical to that for FF-WCE during the early 20th c. but is less during the remainder of the simulation with the largest difference (11.28% of area) during the mid 21st c. (Fig 7A, Table 5). FAB for FS-WCE is similar to that for FF-WCE through the 20th c., but is greater during the 21st c. with the largest difference (2.79% of cell area) during the mid 21st c. (Fig 7B, Table 5). TAB for FS-WCE is identical to that for FF-WCE during the early 20th c., but lower during all other periods, with the largest difference (0.29% of area) during the mid 21st c. (Fig 7C, Table 5).

AWF is consistently lower for SF-WCE than for FF-WCE during the entire simulation with the greatest difference (24.34% of area) during the late 21st c. (Fig 7A, Table 5). FAB is consistently higher for SF-WCE than for FF-WCE throughout the simulation with the greatest difference (49.71% of area) occurring in the early 20th c. (Fig 7B, Table 5). TAB is initially higher for SF-WCE than for FF-WCE during the early and mid 20th c. (largest difference of 0.28% of area during mid 20th c.) but is lower for the remainder of the simulation (largest difference of 0.60% of area during the mid 21st c.; Fig 7B, Table 5).

Carbon fluxes

For WCE scenarios, NPP increases by approximately 5% over the 20th c. and an additional 18% over the 21st c. (Fig 8A, Table 6). NPP varies by less than 3% across all WCE scenarios within any time period. For FF-NCE, NPP does not vary over the 20th c. but decreases by 10% over the 21st c. (Fig 8A, Table 6). NPP for NF-NCE increases by 1% over the 20th c. and decreases by 8% over the 21st c. (Fig 8A, Table 6).

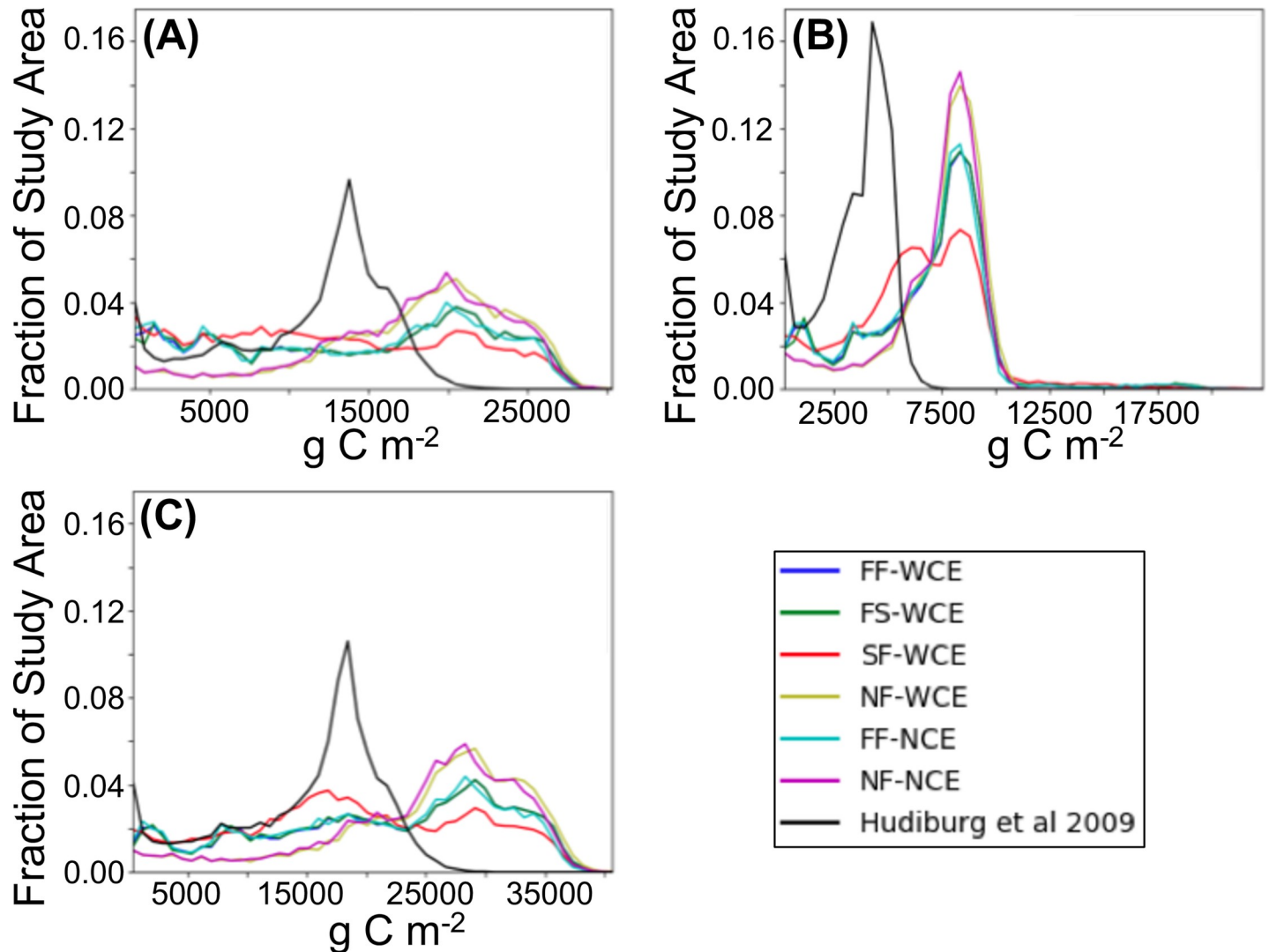


Fig 5. Simulated carbon density distributions by the MC2 vegetation model for natural areas as a fraction of the entire study area. (A) AGB (above ground live woody biomass), (B) AGD (above ground dead woody carbon), and (C) AGT (above ground total woody carbon).

<https://doi.org/10.1371/journal.pone.0210989.g005>

Over the simulation period, NEP increases for WCE scenarios and decreases for both NCE scenarios (Fig 8B, Table 6). Throughout the simulation period, for FF-WCE and FF-NCE, NEP increases more than for their no-fire counterparts (Fig 8B, Table 6).

Consumed C for with-fire scenarios (FF-WCE, FS-WCE, FF-NCE) is nearly identical during the 20th c. (Fig 8C, Table 6). For these scenarios, consumed C triples from the late 20th c. to the late 21st c. The pattern of consumed C is similar among these scenarios throughout the 21st c., but the range of values increases by the end of the 21st c. For SF-WCE, consumed C is higher than that for FF-WCE over the 20th c. but lower during the 21st c. The standard deviation of SF-WCE consumed C is higher than that for FF-WCE during the early and mid 20th c. but lower during the late 20th c. and the mid 21st c. (Table 6).

During the early and mid 20th c. NBP is lower for SF-WCE than that for all other scenarios but becomes higher than that for all scenarios except NF-WCE by the end of the 21st c. (Fig 8D, Table 6). NBP for SF-WCE shows much less variability than FF-WCE in the mid and late

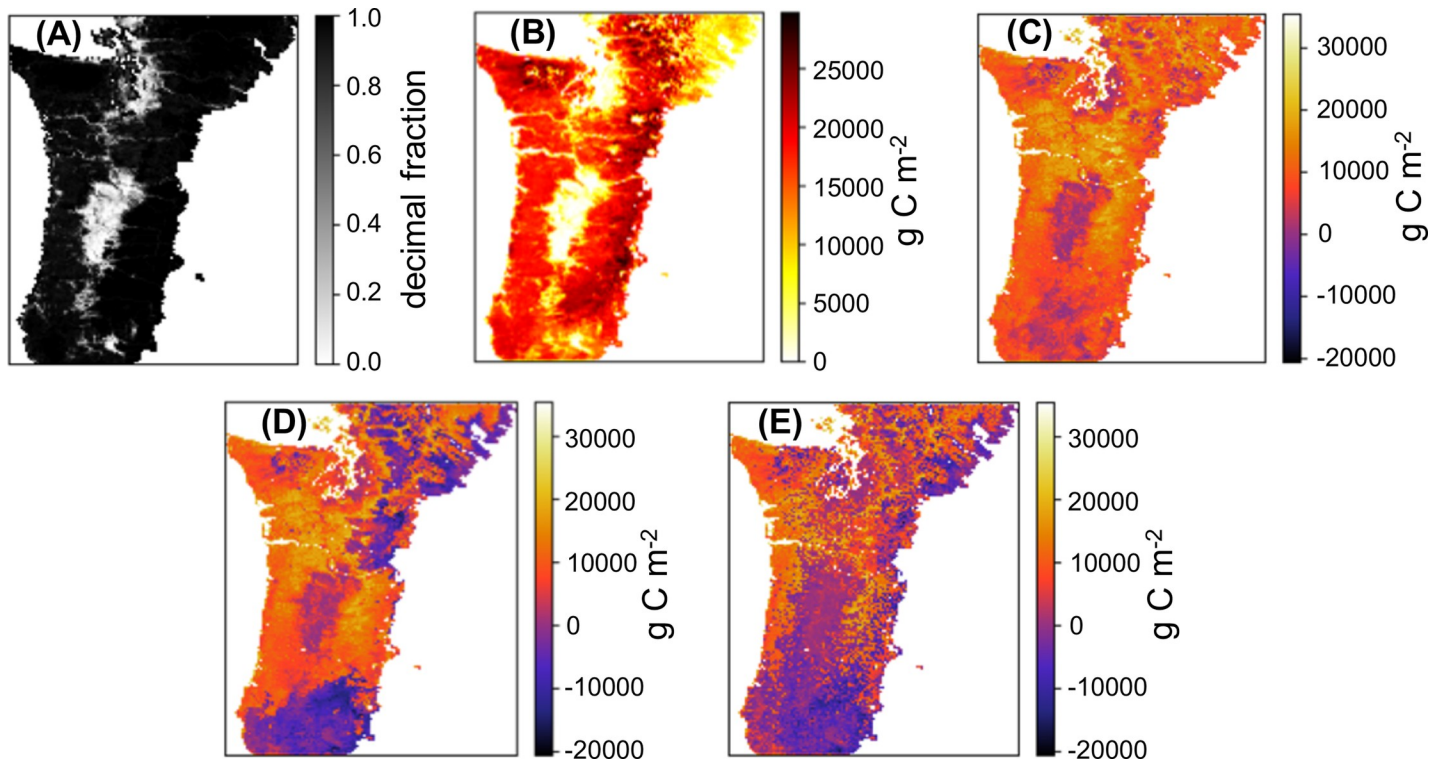


Fig 6. Human affected areas and carbon measures over the study area. (A) Density of NHA (non-human-affected) area used to calculate carbon densities. (B) AGT (aboveground total woody biomass) densities derived from [37] for 1991–1999. (C–E) Differences in carbon densities calculated by subtracting Hudiburg’s results from simulation results for 1991–1999: (C) NF-WCE (no fire, with CO₂ fertilization effect); (D) FF-WCE (full fire, with CO₂ fertilization effect) (E) SF-WCE (stochastic fire, with CO₂ fertilization effect).

<https://doi.org/10.1371/journal.pone.0210989.g006>

21st c. NBP for FF-WCE and FS-WCE falls sharply from the late 20th c. to the mid 21st c. but rises during the late 21st c. NBP for FF-NCE decreases more abruptly from the late 20th c. to the mid 21st c. and increases less during the late 21st c. NBP for NF-WCE increases from the late 20th to the mid 21st c. then decreases during the late 21st c. NBP for NF-NCE decreases from the late 20th c. through the mid and late 21st c.

Carbon pools

Live C (C in live plants), dead C (standing dead trees, litter, and soil C), and total ecosystem C (ecosystem C hereafter) for NF-WCE increase throughout the simulation by 4, 6, and 10% respectively, with the live to dead C ratio decreasing from 0.65 to 0.61 (Fig 9A–9D, Table 7). For FF-WCE and FS-WCE live C decreases 7.5% from the late 20th c. to the late 21st c. (Fig 9A, Table 7). Over the same period dead C pools increase 4 and 6% for FF-WCE and FS-WCE respectively, and ecosystem C decreases 7% for both scenarios, and live to dead ratios decrease from 0.56 to 0.39 and 0.56 to 0.38 for FF-WCE and NF-WCE respectively (Fig 9A–9D, Table 7). For FF-NCE, live, dead C, and ecosystem C decrease by 41, 12, and 22% respectively from the late 20th c. through the late 21st c. and the live to dead C ratio decreases (from 0.56 to 0.38; Fig 9A–9D, Table 7).

For SF-WCE, live C decreases by 16% from the early 20th c. to the mid 20th c., dead C increases 7% from the late 20th to the late 21st c., and ecosystem C decreases by 2% from the early 20th to the late 21st c. (Fig 9A–9C, Table 7). Over the same period, the live to dead C ratio decreases from 0.55 to 0.42 (Fig 9D, Table 7).

Table 4. Carbon flux and pool values from other studies and the current study.

Source	Period	Method	NPP (gCm ⁻² yr ⁻¹)	NEP (gCm ⁻² yr ⁻¹)	NBP or NECB (gCm ⁻² yr ⁻¹)	C stocks (gCm ⁻²)	Comments
[38] ¹	1986–2010	Biome BGC informed by field and remote sensing observations		~100 to ~200			Includes harvest, fire, and land cover
[14] ²	1986–2010	Biome BGC informed by field and remote sensing observations	~600 to ~800	~0 to ~-600	~22 to ~67		West Cascades ecoregion only; study includes fire, timber harvest, land use, and pests
[39] ³	1980–1997	Biome BGC informed by field and remote sensing observations	640 to 700	190 to 226	1684	32810 to 38810	Forested areas within western OR; includes fire and harvest
[37] ⁵	1991–1999	Biome BGC informed by field observations	540 to 820 (~1200 to ~1500)			32810 to 46800 (~58000 to 84000)	OR and Northern CA, C Stocks are for above ground live and dead carbon including only trees and shrubs.
FF-WCE	1971–2000		1198	52	19	54400	
FS-WCE	1971–2000		1198	52	21	54500	
SF-WCE	1971–2000		1199	65	20	50900	
NF-WCE	1971–2000		1214	29	29	59700	
FF-NCE	1971–2000		1136	19	-13	53300	
NF-NCE	1971–2000		1152	-2	-3	58500	

(FF-WCE: full fire, with CO₂ fertilization effect; FS-WCE: with fire suppression, with CO₂ fertilization effect; SF-WCE: with stochastic ignitions, with CO₂ fertilization effect; NF-WCE: no fire, with CO₂ fertilization effect; FF-NCE: full fire, with no fertilization effect; and NF-NCE: no fire, with no CO₂ fertilization effect. ¹NEP values included for only for those ecoregions within our study area; ²NECB listed in table, calculated as NEP minus fire emissions minus simulated harvest removals; ³Values included for only forested lands in areas falling within our study area; ⁴Value is for all of forested western Oregon, reported as NBP; ⁵Oregon and northern California, values are the maximum versus stand age, values are from central trend line of data with maximum values in parentheses).

<https://doi.org/10.1371/journal.pone.0210989.t004>

Vegetation

Vegetation composition is consistent across all scenarios, with the differences of 3% or less for all categories in each time period (Fig 10, Table 8). The *other* category (non-forest) comprises two percent or less of the area from the early 20th c. through the late 21st c. Through the 20th c., conifer covers between 88% to 94% of the area with temperate mixed forest accounting for the remainder of the forested area. From the late 20th to mid 21st c. conifer forest extent decreases to 53 to 55% of the area, temperate mixed forest increases to 39 to 40%, and subtropical mixed forest increases to 5% of the area. During the late 21st c. conifer forest extent decreases to 34 to 35%, temperate mixed forest decreases to 32%, and subtropical mixed forest increases to 33% of the area.

Discussion

Validation, comparison with other studies, and limitations

For unlimited ignition scenarios versus observed fires there is general agreement between areas where area burned is greatest. The lack of concentrated modeled TAB in the southwest corner of the region versus observed (Fig 4C vs 4B) may be due to the use of a dataset with

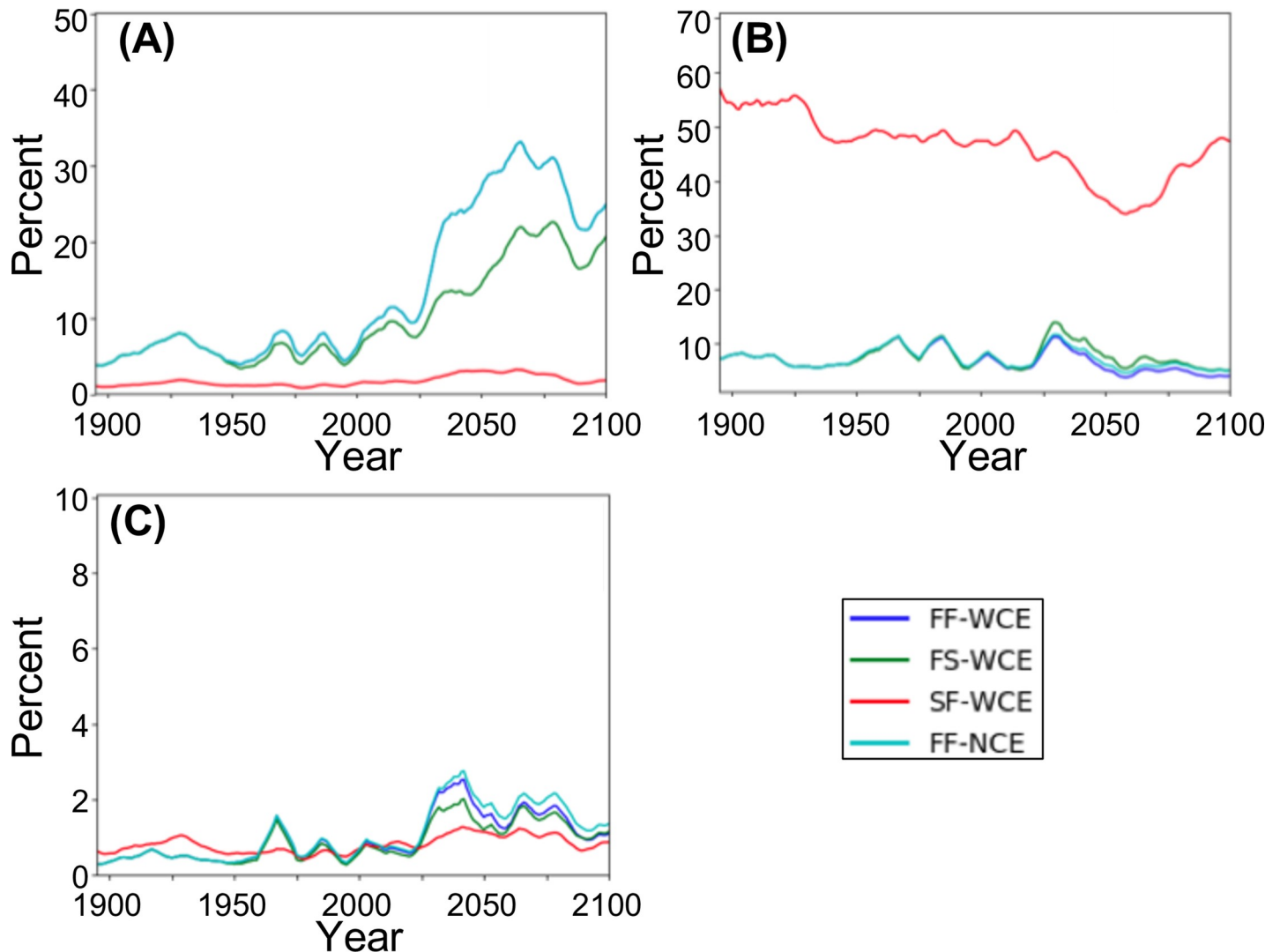


Fig 7. Fire results by scenario as a percentage of total area. (A) AWF (Area with fire; the area of all grid cells experiencing any fire); (B) FAB (Fraction area burned; the fraction of are burned in grid cells with fire); and (C) TAB (Total area burned; the sum of (AWF * FAB) over all grid cells). (FF-WCE: full fire, with CO₂ fertilization effect; FS-WCE: with fire suppression, with CO₂ fertilization effect; SF-WCE: with stochastic ignitions, with CO₂ fertilization effect; and FF-NCE: full fire, with no fertilization effect. Results smoothed using triangle smoothing +/- 8 years).

<https://doi.org/10.1371/journal.pone.0210989.g007>

deeper soils than are actually present. In the model, shallower soils retain less water, potentially leading to drier fuel conditions and greater fire. In this part of the study area, the STATSGO dataset used in the simulation has soil depths two to four times as deep as the more recent SSURGO dataset [40].

The overall higher simulated TAB and the higher simulated TAB east of Puget Sound—primarily due to simulated fires in 1987 and 2003—underscore the importance of modeling wild-fire ignition limitations in addition to fuel limitations. Stochastic fire (SF) mitigates the overall higher TAB, but simulates more fires than observed in areas that are commonly fuel limited (Cascades and Coast range). The stochastic ignitions algorithm used in the SF-WCE scenario was implemented as a proof of concept with a random algorithm to locate ignition sources. An algorithm using a probability surface based on factors affecting ignition sources such as human presence and infrastructure (e.g. [41–42]) and lightning strikes (e.g. [43–44]) would

Table 5. Summaries of fire characteristics over the study area.

1895–1924	AWF (%)	FAB (%)	TAB (%)
FF-WCE	5.31	8.95	0.48
FS-WCE	5.31	8.95	0.48
SF-WCE	1.25	58.66	0.73
FF-NCE	5.31	8.95	0.48
1936–1965	AWF (%)	FAB (%)	TAB (%)
FF-WCE	4.62	8.12	0.38
FS-WCE	4.27	7.99	0.34
SF-WCE	1.21	49.44	0.60
FF-NCE	4.62	8.19	0.38
1971–2000	AWF (%)	FAB (%)	TAB (%)
FF-WCE	5.94	9.43	0.56
FS-WCE	4.88	9.70	0.47
SF-WCE	1.08	49.46	0.53
FF-NCE	5.94	9.64	0.57
2036–2065	AWF (%)	FAB (%)	TAB (%)
FF-WCE	26.93	6.47	1.74
FS-WCE	15.65	9.26	1.45
SF-WCE	2.97	38.26	1.14
FF-NCE	26.93	7.38	1.99
2071–2100	AWF (%)	FAB (%)	TAB (%)
FF-WCE	26.36	5.03	1.33
FS-WCE	19.90	6.37	1.27
SF-WCE	2.02	43.88	0.89
FF-NCE	26.36	6.11	1.61

Mean annual percentage of AWF (area with fire; area of gridcells in which fire occurred); FAB (fraction area burned; area weighted mean of the fraction of burning in burned grid cells); and TAB (total area burned; AWF * FAB). (FF-WCE: full fire, with CO₂ fertilization effect; FS-WCE: with fire suppression, with CO₂ fertilization effect; SF-WCE: with stochastic ignitions, with CO₂ fertilization effect; and FF-NCE: full fire, with no fertilization effect)

<https://doi.org/10.1371/journal.pone.0210989.t005>

likely produce more realistic results but this kind of data is lacking both for the beginning of 20th century and for the 21st century. Secondly, informing the algorithm with known relationships between fuel conditions and fire initiation would likely also improve results. Additionally, considering conditions more or less conducive to fire initiation, such as slope and other topographic characteristics could also contribute to higher quality fire modeling. Multiple model runs with stochastic ignition sources and success should also be considered to generate a statistics-based projection of fire on the landscape.

Differences between our results and those of other studies (Table 4) are due to a number of factors. First, observation-based models generally only consider aboveground stocks, while MC2 models above- and belowground carbon, including soils and litter. Second, other studies include disturbances that MC2 does not, for example logging, insect infestations, and disease, which would account for some of the higher carbon stock value in our results. Third, the mapping of human-affected (HA) areas reduces differences due to land use, but HA areas can only be considered a first approximation of human influences on the landscape, including historical logging in areas now recovering and fires not accounted for in the simulation, (e.g. the Tillamook fire; [45]).

Our results contrast with [46], which projects increasing forest carbon stocks in Oregon forests through the 21st c. That study assumes a CO₂ fertilization effect. However, unlike ours,

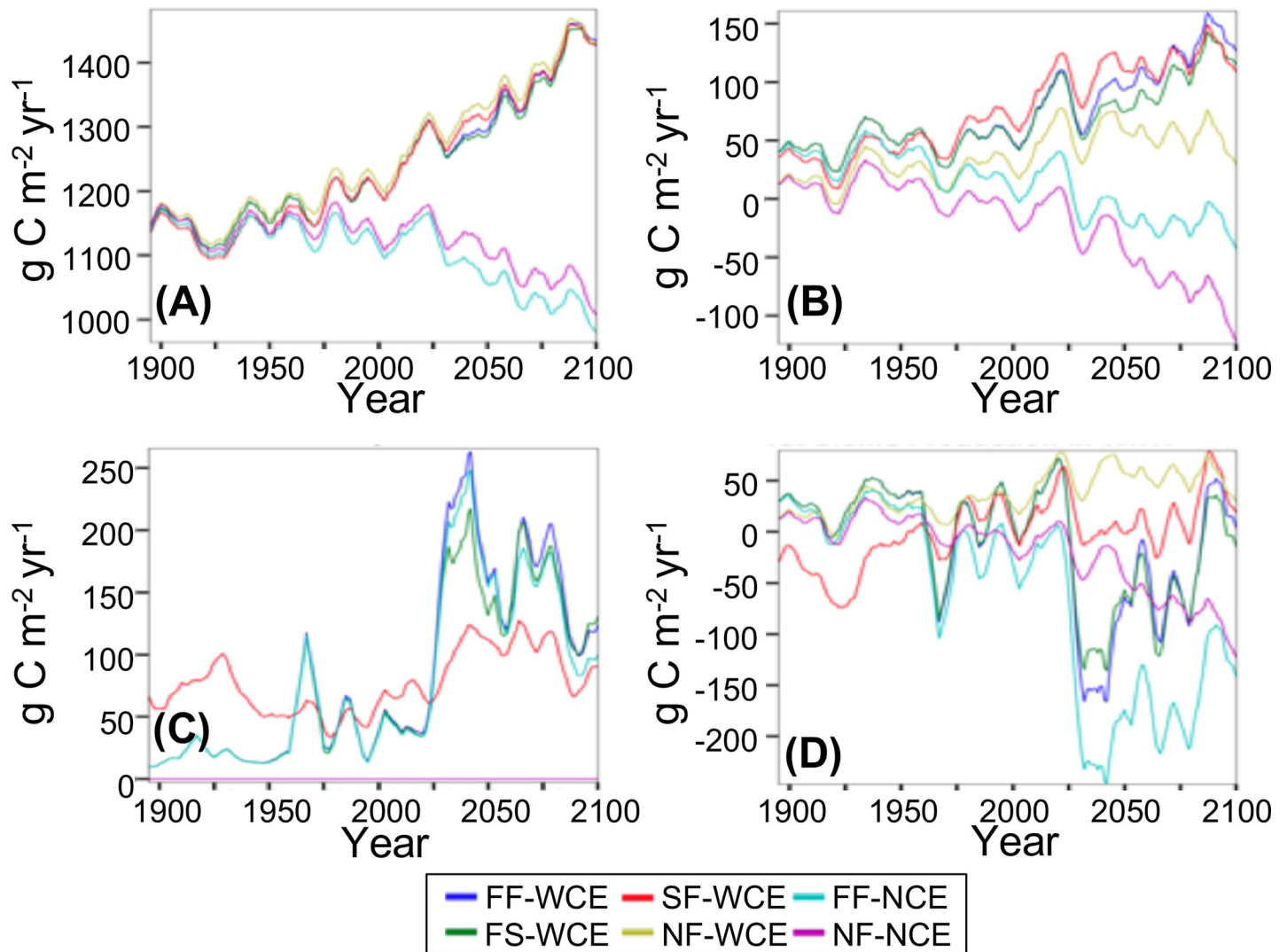


Fig 8. Carbon fluxes simulated by the MC2 vegetation model. (A) NPP (net primary production), (B) NEP (net ecosystem production), (C) C consumed by fire, and (D) NBP (net biome production). (FF-WCE: full fire, with CO₂ fertilization effect; FS-WCE: with fire suppression, with CO₂ fertilization effect; SF-WCE: with stochastic ignitions, with CO₂ fertilization effect; NF-WCE: no fire, with CO₂ fertilization effect; FF-NCE: full fire, with no fertilization effect; and NF-NCE: no fire, with no CO₂ fertilization effect. Results smoothed using triangle smoothing +/- 8 years).

<https://doi.org/10.1371/journal.pone.0210989.g008>

that study includes mortality from forest harvest and beetles and also assumes the same vegetation that is lost regrows at its maximum potential.

MC2 simulates potential vegetation most adapted to climate inputs. However, vegetation can endure under suboptimal conditions, slowing the replacement of one vegetation type by another, remaining until a sudden disturbance or mortality due to crossing a physiological threshold allows for rapid change. Moreover, MC2 does not simulate seed production, seedling establishment, or natural succession. These factors should be accounted for when using model projections for management decisions.

Land use, insects, pathogens, and invasive species are important disturbances that may be amplified or mitigated by climate change (e.g. [47–49]). Including them in the DGVM is desirable, but would require a better understanding of a wide variety of pests’ and invasive species’ response to climate change as well as calibration datasets that are still often lacking.

Table 6. Mean (standard deviation in parentheses) carbon fluxes by time period for simulation scenarios.

NPP (g C m ⁻² yr ⁻¹)					
	1895–1924	1936–1965	1971–2000	2036–2065	2071–2100
FF-WCE	1143 (79)	1173 (94)	1198 (87)	1315 (132)	1422 (136)
FS-WCE	1143 (79)	1173 (94)	1198 (87)	1307 (130)	1413 (134)
SF-WCE	1131 (79)	1156 (92)	1199 (87)	1329 (133)	1420 (133)
NF-WCE	1150 (80)	1179 (94)	1214 (87)	1344 (131)	1430 (130)
FF-NCE	1136 (80)	1149 (93)	1136 (81)	1072 (122)	1024 (109)
NF-NCE	1143 (80)	1155 (93)	1152 (81)	1111 (126)	1060 (114)
NEP (g C m ⁻² yr ⁻¹)					
	1895–1924	1936–1965	1971–2000	2036–2065	2071–2100
FF-WCE	37 (46)	55 (50)	52 (49)	99 (66)	136 (100)
FS-WCE	37 (46)	55 (50)	52 (49)	82 (63)	121 (97)
SF-WCE	27 (46)	48 (49)	65 (50)	115 (67)	126 (96)
NF-WCE	10 (46)	27 (49)	29 (49)	62 (62)	54 (92)
FF-NCE	32 (46)	42 (49)	19 (44)	-12 (61)	-19 (76)
NF-NCE	5 (46)	14 (48)	-3 (44)	-40 (63)	-82 (80)
Consumed (g C m ⁻² yr ⁻¹)					
	1895–1924	1936–1965	1971–2000	2036–2065	2071–2100
FF-WCE	20 (32)	15 (19)	34 (55)	177 (217)	145 (139)
FS-WCE	20 (32)	15 (18)	31 (52)	155 (199)	139 (132)
SF-WCE	71 (51)	53 (36)	45 (30)	112 (72)	92 (48)
NF-WCE	0 (0)	0 (0)	0 (0)	0 (0)	0 (0)
FF-NCE	20 (32)	15 (18)	33 (54)	169 (200)	126 (124)
NF-NCE	0 (0)	0 (0)	0 (0)	0 (0)	0 (0)
NBP (g C m ⁻² yr ⁻¹)					
	1895–1924	1936–1965	1971–2000	2036–2065	2071–2100
FF-WCE	17 (61)	40 (56)	19 (87)	-77 (257)	-7.9 (214)
FS-WCE	17 (61)	40 (56)	21 (85)	-73 (238)	-18 (207)
SF-WCE	-44 (71)	-5 (70)	20 (64)	3 (126)	34 (122)
NF-WCE	10 (46)	27 (49)	29 (49)	62 (62)	54 (92)
FF-NCE	12 (61)	27 (55)	-13 (81)	-181 (233)	-144 (174)

(Continued)

Table 6. (Continued)

NF-NCE	5 (46)	14 (48)	-3 (43)	-40 (63)	-82 (80)
--------	-----------	------------	------------	-------------	-------------

(NPP: net primary production; NEP: net ecosystem production; NBP: net biome production; FF-WCE: full fire, with CO₂ fertilization effect; FS-WCE: with fire suppression, with CO₂ fertilization effect; SF-WCE: with stochastic ignitions, with CO₂ fertilization effect; NF-WCE: no fire, with CO₂ fertilization effect; FF-NCE: full fire, with no fertilization effect; and NF-NCE: no fire, with no CO₂ fertilization effect)

<https://doi.org/10.1371/journal.pone.0210989.t006>

Soil data are critical for projecting accurate soil water availability and drought stress [40]. More accurate soil data would improve the reliability of growth, mortality, and fire simulation results. More recent MC2 simulations have used SSURGO data but at the time of this project, the dataset was still incomplete for large portions of our study area.

Effects of model assumptions on vegetation

The simulated transition from conifer to temperate mixed conifer/broadleaf to subtropical mixed conifer/broadleaf takes place at a similar rate and with a similar pattern regardless of fire and CO₂ fertilization and can be attributed solely to climate change. Other studies using MC2 and its predecessor, MC1, project vegetation shifts in this region towards warmer and mixed forests [1–2, 14, 50], however, to our knowledge, ours is the first study to show that this shift is purely climate driven. This result stands in contrast to the simulated fire regime-driven vegetation shifts in other regions found in other studies using MC2 (e.g. [1, 31])

Effects of model assumptions on fire

With or without fire suppression, unlimited ignitions cause a sharp increase in AWF as climate conditions drive fuel conditions over ignition thresholds on a yearly basis during the early and mid 21st c. This is consistent with recent observed increases in wildfire across the western US, including the PNW, due to warming climate [3, 51] and specifically in the Western Cascades due to decreased May through September precipitation [52]. The initial decrease in FAB and TAB as AWF remains high is due to the dependency of FAB on the combination of time since last fire and fire return interval (FRI) in addition to fuel conditions. The longer a cell does not burn, the greater the fraction of that cell that can burn. With the initial transition to more frequent fires, the first fire in a cell burns a greater cell portion than subsequent fires in the same cell. The vegetation shift to subtropical mixed forest, which has a higher ignition threshold, contributes to decreased AWF, FAB, and TAB towards the end of the 21st c. The higher fuel thresholds of fire suppression reduce AWF and TAB due to fuel conditions reaching ignition thresholds less frequently. Less frequent fires, however, account for the greater TAB under fire suppression.

Stochastic fire responds to the same drivers as the unlimited ignitions but in different ways. First, the use of an ignition probability function instead of a single fuel threshold allows fires to occur even under fuel conditions less severe than those at unlimited ignition threshold levels. Thus, during the early 20th c. some cells not experiencing fire under unlimited ignitions do experience fire under stochastic ignitions leading to a greater TAB under stochastic fire. Second, the probabilistic nature of ignition sources and fire initiation limits fire occurrence under fuel conditions exceeding thresholds, as during the early to late 21st c. when fire occurrence is more common across the entire study area under unlimited ignitions than under stochastic fire. During this period, TAB is lower under stochastic fire than under unlimited ignitions

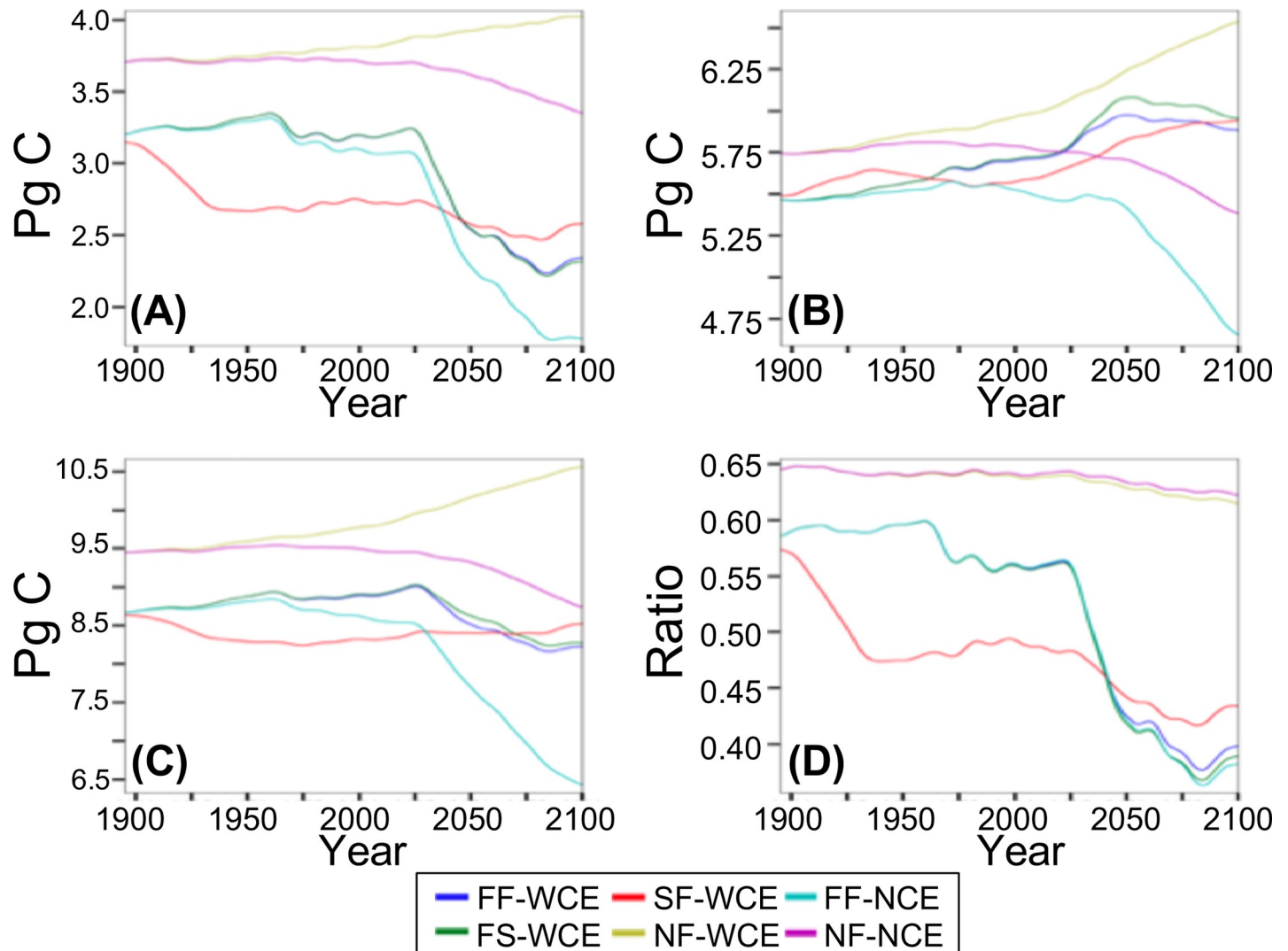


Fig 9. Carbon pools and live/dead ratios. (A) live C, (B) dead C, (C) ecosystem C, and (D) ratio of live C to dead C. (FF-WCE: full fire, with CO₂ fertilization effect; FS-WCE: with fire suppression, with CO₂ fertilization effect; SF-WCE: with stochastic ignitions, with CO₂ fertilization effect; NF-WCE: no fire, with CO₂ fertilization effect; FF-NCE: full fire, with no fertilization effect; and NF-NCE: no fire, with no CO₂ fertilization effect. Results smoothed using triangle smoothing +/- 8 years).

<https://doi.org/10.1371/journal.pone.0210989.g009>

scenarios due to less frequent fire occurrence. The overall less frequent fires due to stochastic fire result in a lower AWF and higher FAB. Stochastic fire occurring below the thresholds set for unlimited ignitions accounts for the higher FAB at the end of the 21st c., when stochastic fire initiates fires in subtropical mixed forest while unlimited ignitions does not.

Fire effects due to CO₂ fertilization assumptions are generally small. However, even though AWF is identical for FF-NCE and FF-WCE, FAB and TAB are slightly higher for FF-NCE. We attribute this to dryer fuel conditions as a result of lower water use efficiency (WUE) for FF-NCE.

Effects of model assumptions on carbon

Separate from fire, CO₂ fertilization under climate change increases productivity and C in all pools through time. Conversely the lack of CO₂ fertilization under climate change decreases productivity C in all pools. The smooth changes in C pools and ratio of live to dead C for both

Table 7. Mean (standard deviation in parentheses) carbon pool values and live to dead C ratios by time period.

Live Carbon (Pg)					
	1895–1924	1936–1965	1971–2000	2036–2065	2071–2100
FF-WCE	3.24 (0.025)	3.32 (0.033)	3.18 (0.032)	2.60 (0.149)	2.30 (0.059)
FS-WCE	3.24 (0.025)	3.32 (0.033)	3.18 (0.032)	2.60 (0.151)	2.28 (0.058)
SF-WCE	3.03 (0.104)	2.66 (0.017)	2.72 (0.037)	2.59 (0.053)	2.52 (0.048)
NF-WCE	3.72 (0.014)	3.75 (0.019)	3.79 (0.020)	3.93 (0.025)	4.00 (0.024)
FF-NCE	3.23 (0.024)	3.29 (0.027)	3.12 (0.036)	2.33 (0.186)	1.83 (0.078)
NF-NCE	3.72 (0.014)	3.72 (0.014)	3.72 (0.011)	3.61 (0.037)	3.43 (0.053)
Dead Carbon (Pg)					
	1895–1924	1936–1965	1971–2000	2036–2065	2071–2100
FF-WCE	5.47 (0.015)	5.56 (0.019)	5.67 (0.024)	5.95 (0.037)	5.91 (0.024)
FS-WCE	5.47 (0.015)	5.56 (0.019)	5.68 (0.026)	6.04 (0.050)	6.00 (0.033)
SF-WCE	5.54 (0.042)	5.62 (0.022)	5.56 (0.015)	5.81 (0.049)	5.92 (0.015)
NF-WCE	5.75 (0.014)	5.85 (0.018)	5.92 (0.027)	6.24 (0.063)	6.46 (0.052)
FF-NCE	5.47 (0.012)	5.52 (0.009)	5.55 (0.020)	5.38 (0.100)	4.87 (0.150)
NF-NCE	5.75 (0.011)	5.80 (0.008)	5.79 (0.010)	5.67 (0.030)	5.48 (0.069)
Total Ecosystem Carbon (Pg)					
	1895–1924	1936–1965	1971–2000	2036–2065	2071–2100
FF-WCE	8.70 (0.028)	8.88 (0.049)	8.85 (0.026)	8.54 (0.124)	8.21 (0.052)
FS-WCE	8.71 (0.028)	8.88 (0.050)	8.87 (0.027)	8.64 (0.110)	8.28 (0.052)
SF-WCE	8.57 (0.064)	8.29 (0.016)	8.28 (0.032)	8.40 (0.017)	8.44 (0.054)
NF-WCE	9.47 (0.017)	9.60 (0.033)	9.71 (0.042)	10.2 (0.083)	10.5 (0.072)
FF-NCE	8.70 (0.023)	8.81 (0.032)	8.67 (0.033)	7.71 (0.263)	6.69 (0.213)
NF-NCE	9.46 (0.013)	9.52 (0.016)	9.51 (0.007)	9.30 (0.063)	8.91 (0.120)
Live / Dead (ratio)					
	1895–1924	1936–1965	1971–2000	2036–2065	2071–2100
FF-WCE	0.59 (0.005)	0.60 (0.004)	0.56 (0.007)	0.44 (0.027)	0.39 (0.011)
FS-WCE	0.59 (0.005)	0.60 (0.004)	0.56 (0.008)	0.43 (0.028)	0.38 (0.011)
SF-WCE	0.55 (0.023)	0.48 (0.005)	0.49 (0.008)	0.45 (0.013)	0.42 (0.008)
NF-WCE	0.65 (0.003)	0.64 (0.003)	0.64 (0.003)	0.63 (0.004)	0.61 (0.003)
FF-NCE	0.59 (0.005)	0.60 (0.005)	0.56 (0.007)	0.43 (0.030)	0.38 (0.011)

(Continued)

Table 7. (Continued)

NF-NCE	0.65 (0.003)	0.64 (0.003)	0.64 (0.003)	0.64 (0.005)	0.63 (0.003)
--------	-----------------	-----------------	-----------------	-----------------	-----------------

(Pg: petagram; FF-WCE: full fire, with CO₂ fertilization effect; FS-WCE: with fire suppression, with CO₂ fertilization effect; SF-WCE: with stochastic ignitions, with CO₂ fertilization effect; NF-WCE: no fire, with CO₂ fertilization effect; FF-NCE: full fire, with no fertilization effect; and NF-NCE: no fire, with no CO₂ fertilization effect)

<https://doi.org/10.1371/journal.pone.0210989.t007>

no-fire scenarios indicate little change in carbon dynamics. The continuing increases in all C pools for NF-WCE and decreases for NF-NCE indicate that climate continues to influence production through the end of the 21st c.

CO₂ fertilization is the strongest driver of NPP as shown by the similar increases in NPP across all scenarios with CO₂ fertilization versus the similar decrease for scenarios without CO₂ fertilization. Consumed C is very similar for all scenarios with unlimited ignitions. Increased carbon storage in young forests recovering from fire as well as to the reduction of dead material available for decomposition due to burning drive higher NEP for all scenarios with CO₂ fertilization and unlimited ignitions. However, for FF-NCE, NEP decreases due to decreasing NPP.

For scenarios with unlimited ignitions, consumed C directly reflects TAB increasing sharply in the mid 20th c. and then decreasing. This pattern is further reflected in NBP which decreases and increases with TAB. By the end of the 21st c., NBP is close to 0 g C m⁻² yr⁻¹ for scenarios with unlimited ignitions and with CO₂ fertilization, indicating a possible equilibrium in carbon dynamics. However, for FF-NCE, NBP remains negative, indicating further C losses.

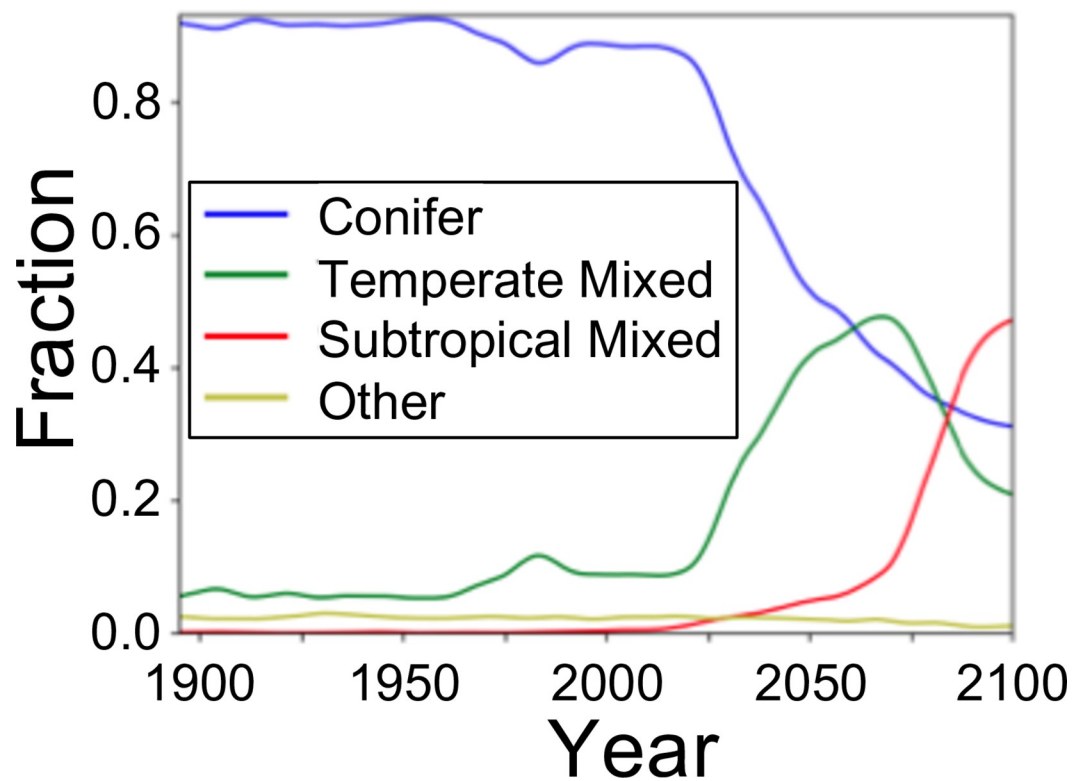


Fig 10. Vegetation class mix over time for FF-WCE (full fire with CO₂ fertilization) scenario. All other scenarios yield virtually identical results.

<https://doi.org/10.1371/journal.pone.0210989.g010>

Table 8. Simulated vegetation composition (%) of study area.

1895–1924	Con	T Mix	S Mix	Oth
FF-WCE	92	6	0	2
FS-WCE	92	6	0	2
SF-WCE	92	6	0	2
NF-WCE	94	6	0	0
FF-NCE	92	6	0	2
NF-NCE	94	6	0	0
1936–1965	Con	T Mix	S Mix	Oth
FF-WCE	93	5	0	2
FS-WCE	93	5	0	1
SF-WCE	92	5	0	2
NF-WCE	94	5	0	0
FF-NCE	93	5	0	2
NF-NCE	94	5	0	0
1971–2000	Con	T Mix	S Mix	Oth
FF-WCE	88	10	0	2
FS-WCE	88	10	0	2
SF-WCE	88	10	0	2
NF-WCE	90	10	0	0
FF-NCE	87	10	0	3
NF-NCE	90	10	0	0
2036–2065	Con	T Mix	S Mix	Oth
FF-WCE	54	40	5	2
FS-WCE	53	40	5	3
SF-WCE	53	40	5	2
NF-WCE	55	40	5	0
FF-NCE	53	39	5	3
NF-NCE	55	40	5	0
2071–2100	Con	T Mix	S Mix	Oth
FF-WCE	35	32	33	0
FS-WCE	34	32	33	1
SF-WCE	34	32	33	1
NF-WCE	35	32	33	0
FF-NCE	34	32	33	1
NF-NCE	35	32	33	0

(Con: conifer; T Mix: temperate mixed conifer and broadleaf; S Mix: subtropical mixed conifer and broadleaf; Oth: other; Veg: vegetation; FF-WCE: full fire, with CO₂ fertilization effect; FS-WCE: with fire suppression, with CO₂ fertilization effect; SF-WCE: with stochastic ignitions, with CO₂ fertilization effect; NF-WCE: no fire, with CO₂ fertilization effect; FF-NCE: full fire, with no fertilization effect; and NF-NCE: no fire, with no CO₂ fertilization effect)

<https://doi.org/10.1371/journal.pone.0210989.t008>

For SF-WCE, consumed C and NBP also reflect TAB, with consumed C greater than that for unlimited-ignitions scenarios in the early 20th c. and less during the mid and late 21st c.

More live C is lost due to fire than is added due to CO₂ fertilization. For unlimited ignitions, losses are greatest during the mid to late 21st c. when fuel thresholds are exceeded. For stochastic fire, the greatest losses are in the early 20th c. due to fires occurring where they cannot under unlimited ignitions. CO₂ fertilization, however, may provide enough productivity to maintain a new equilibrium with increased dead C and limited decreases in ecosystem C. For

all with-CO₂ fertilization, with-fire scenarios, at the end of the 21st c., the steady values of all C stocks and live to dead C ratios indicate the possibility of a new equilibrium. This is consistent with the near 0 g C m⁻² yr⁻¹ NBP for these scenarios at the end of the 21st c.

The largest decreases in all C stocks are for the with-fire, without-CO₂ fertilization. In addition, while live vegetation C becomes steady for this scenario at the end of the 21st c., dead C, and ecosystem C continue to decrease, indicating that equilibrium has not been reached. This is consistent with the negative NBP for this scenario at the end of the 21st c.

Implications

The sharp, climate-driven increases in area with fire and total area burned during the first half of the 21st suggest this region will be susceptible to climate-driven trend towards “large,” “very large,” or “extreme” wildfire events or fires [53] observed in the United States [54, 55], Europe [56, 57], and globally [58]. The increases also indicate that this region will experience the associated increases in infrastructure loss, suppression costs, and natural resource loss [59], and underscore the importance of understanding the effects of alternative management scenarios in fire-prone landscapes [60].

The live C lost in all with-fire scenarios indicates fire will cause mortality through the 21st c. Another indication of future vegetation mortality is the climate-driven transition from needle-leaf to temperate mixed to warm mixed forest. MC2 does not simulate mortality, seeding, sprouting, recruitment, and succession associated with forest type change driven by climate alone. So, for example, under a warming climate, the model could shift a forest dominated by needleleaf lifeforms to one dominated by mixed conifer and hardwood lifeforms without simulating mortality and succession. Thus, model results should be interpreted as a suggestion that vegetation will come under stress due to a changing climate. Mortality and vegetation type change would not necessarily be sudden. However, stressed vegetation would be more susceptible to disturbances [48] such as drought, fire, insects [49, 61], and disease, with the resulting mortality providing opportunity for vegetation to change from legacy to a more suited type.

Shorter FRIs combined with reduced recruitment due to changed climate conditions has the potential to extirpate species locally [62]. Furthermore, climate change velocity, especially in combination with pest outbreaks, could outpace species' migration rates [63], leaving portions of the area depauperate. The subtropical mixed forests projected to occupy much of the area by the end of the 21st c. are characterized by both needleleaf and broadleaf evergreens and would be similar to northern Californian forests which contain evergreen California live oaks (*Quercus agrifolia*). However, the decline of oak populations due to sudden oak death syndrome (*Phytophthora ramorum*) in California and Oregon [64] challenges any assumption of a northward migration of this evergreen broadleaf species.

Ecosystem C decreases in all with-fire scenarios indicate that this region will become a carbon source in the future. Decreases may be more pronounced beyond 2100 if the increased C in the dead pool decays at a greater rate than dead C is produced. This is possible as the simulated increase in dead C is due to a sudden increase in fire in forests that had been highly productive, and the live to dead C ratios increase towards previous equilibrium values at the end of the simulation. If the CO₂ effect is lower than projected or is temporary, with plants adapting to the new CO₂ concentrations, carbon losses may be higher than projected under the WCE scenarios, for example, 1.69 Pg C (20%) greater for the FF-NCE than for the FF-WCE. However black carbon accumulation from more frequent fire and the possible slowing of decomposition due to higher evaporative demand in soils may mitigate losses of soil C.

Under our projections, a variety of ecosystem services could be impacted. As previously stated, carbon sequestration could be reduced. Widespread mortality would reduce timber

available for harvest, and rapid change of vegetation types could result in a lack of mature trees for harvest. The implied negative impacts on forests could affect fresh water supplies [65], wildlife habitat quality, and recreation.

Conclusions

For the area west of the Cascade Crest in Oregon and Washington, we found assumptions about CO₂ fertilization effects and fire occurrence in the MC2 DVGM have substantial effects on simulated carbon dynamics. Without fire, CO₂ fertilization increases C stocks, while the lack of CO₂ fertilization leads to decreases in C stocks. For scenarios with fire, CO₂ fertilization mitigates projected C losses due to fire, limiting decreases over the 20th and 21st centuries by a factor of 4 versus scenarios without CO₂ fertilization.

Stochastic fire occurrence dampens the sudden increases in area with fire, and total area burned simulated under unlimited ignitions. As a result, C pools are more stable through time under stochastic fire occurrence than under unlimited ignitions. The stark differences between results for unlimited ignitions and those for stochastic fire occurrence point to the need for further research regarding fire occurrence algorithms in DGVMs. Areas for further research include: the addition of ignition source probabilities to guide the location of fire occurrence; fire spread which would allow modeling large fires across grid cells; inclusion of land use and land cover to shape both the occurrence and spread of fire; and the elimination of fire return intervals from fire algorithms in order to model fire occurrence and extent from physical parameters and stochastic events without imposed limitations.

Vegetation is projected to change from predominantly conifer to predominantly mixed conifer and hardwood forests, regardless of CO₂ fertilization and fire effects. With climate, not fire, driving vegetation change, much of the current vegetation can be expected to experience mortality. It is reasonable to anticipate that climate stress will make forests more susceptible disease and pests, which are not modeled by MC2.

These projections underscore ongoing challenges for resource managers who must balance the possibly competing concerns of wildfire, forest condition, wildlife management, carbon sequestration, high potential for vegetation change, and a variety of ecosystem services including clean water and air. Nonetheless, this study and its conclusions should be taken in a broader context. MC2 is one of many models suitable to explore the possible futures of this region. Given the region's ecological and economic importance, extensive monitoring is warranted to provide insight into the state of the forests, possibly confirming or refuting signs of stress, vegetation change, and ecological threshold exceedance.

Supporting information

S1 Table. Reclassifications of MC2 vegetation types.
(DOCX)

S1 Fig. Selected climate results for this study. (A) CCSM4 RCP 8.5 annual and April-September maximum temperature, (B) CCSM4 RCP 8.5 annual and April-September precipitation, and (C) Annual PET calculated by MC2. All results smoothed using triangle smoothing +/- 8 years.
(PDF)

S2 Table. Mean (standard deviation in parentheses) over study region for selected climate variables by time period.
(DOCX)

Acknowledgments

Funding for this research was provided by the U.S. Department of the Interior via the Northwest Climate Science Center through agreement #G12AC20495 within the framework of the research project entitled “Integrated Scenarios of climate, hydrology and vegetation for the Northwest”, P. Mote (Oregon State University) principal investigator.

We acknowledge the World Climate Research Programme’s Working Group on Coupled Modelling, which is responsible for CMIP, and we thank the climate modeling groups for producing and making available their model output. For CMIP, the U.S. Department of Energy’s Program for Climate Model Diagnosis and Intercomparison provides coordinating support and led development of software infrastructure in partnership with the Global Organization for Earth System Science Portals.

The authors wish to acknowledge R. Nemani (NASA) for allowing them free access to the Pleiades NASA supercomputer and John Abatzoglou and Katherine Hegewisch (both of University of Idaho) for providing the downscaled CMIP5 climate data used in this study.

Author Contributions

Conceptualization: Tim Sheehan.

Data curation: Tim Sheehan, Ken Ferschweiler.

Formal analysis: Tim Sheehan.

Funding acquisition: Dominique Bachelet.

Methodology: Tim Sheehan, Dominique Bachelet.

Software: Tim Sheehan, Dominique Bachelet, Ken Ferschweiler.

Supervision: Dominique Bachelet.

Validation: Tim Sheehan.

Visualization: Tim Sheehan.

Writing – original draft: Tim Sheehan.

Writing – review & editing: Tim Sheehan, Dominique Bachelet, Ken Ferschweiler.

References

1. Sheehan T, Bachelet D, Ferschweiler K. Projected major fire and vegetation changes in the Pacific Northwest of the conterminous United States under selected CMIP5 climate futures. *Ecological Modelling*. 2015 Dec 10; 317:16–29.
2. Rogers BM, Neilson RP, Drapek R, Lenihan JM, Wells JR, Bachelet D, Law BE. Impacts of climate change on fire regimes and carbon stocks of the US Pacific Northwest. *Journal of Geophysical Research: Biogeosciences*. 2011 Sep 1; 116(G3). <https://doi.org/10.1029/2011jg001641>
3. Westerling AL, Hidalgo HG, Cayan DR, Swetnam TW. Warming and earlier spring increase western US forest wildfire activity. *science*. 2006 Aug 18; 313(5789):940–3. <https://doi.org/10.1126/science.1128834> PMID: 16825536
4. Kurz WA, Dymond CC, Stinson G, Rampley GJ, Neilson ET, Carroll AL, Ebata T, Safranyik L. Mountain pine beetle and forest carbon feedback to climate change. *Nature*. 2008 Apr; 452(7190):987. <https://doi.org/10.1038/nature06777> PMID: 18432244
5. Mote PW, Parson EA, Hamlet AF, Keeton WS, Lettenmaier D, Mantua N, Miles EL, Peterson DW, Peterson DL, Slaughter R, Snover AK. Preparing for climatic change: the water, salmon, and forests of the Pacific Northwest. *Climatic change*. 2003 Nov 1; 61(1–2):45–88.
6. Fowler D, Steadman CE, Stevenson D, Coyle M, Rees RM, Skiba UM, Sutton MA, Cape JN, Dore AJ, Vieno M, Simpson D. Effects of global change during the 21st century on the nitrogen cycle. *Atmospheric Chemistry and Physics*. 2015 Dec 16; 15(24):13849–93.

7. Chen IC, Hill JK, Ohlemüller R, Roy DB, Thomas CD. Rapid range shifts of species associated with high levels of climate warming. *Science*. 2011 Aug 19; 333(6045):1024–6. <https://doi.org/10.1126/science.1206432> PMID: 21852500
8. Rehfeldt GE, Ferguson DE, Crookston NL. Aspen, climate, and sudden decline in western USA. *Forest Ecology and Management*. 2009 Nov 10; 258(11):2353–64.
9. Rehfeldt GE, Crookston NL, Warwell MV, Evans JS. Empirical analyses of plant-climate relationships for the western United States. *International Journal of Plant Sciences*. 2006 Nov; 167(6):1123–50.
10. Lurgi M, López BC, Montoya JM. Novel communities from climate change. *Philosophical Transactions of the Royal Society of London B: Biological Sciences*. 2012 Nov 5; 367(1605):2913–22. <https://doi.org/10.1098/rstb.2012.0238> PMID: 23007079
11. Williams JW, Jackson ST. Novel climates, no-analog communities, and ecological surprises. *Frontiers in Ecology and the Environment*. 2007 Nov 1; 5(9):475–82.
12. Littell JS, McKenzie D, Kerns BK, Cushman S, Shaw CG. Managing uncertainty in climate-driven ecological models to inform adaptation to climate change. *Ecosphere*. 2011 Sep; 2(9):1–9.
13. Cramer W, Bondeau A, Woodward FI, Prentice IC, Betts RA, Brovkin V, Cox PM, Fisher V, Foley JA, Friend AD, Kucharik C. Global response of terrestrial ecosystem structure and function to CO₂ and climate change: results from six dynamic global vegetation models. *Global change biology*. 2001 Apr; 7(4):357–73.
14. Turner DP, Conklin DR, Bolte JP. Projected climate change impacts on forest land cover and land use over the Willamette River Basin, Oregon, USA. *Climatic change*. 2015 Nov 1; 133(2):335–48.
15. Harris RM, Remenyi TA, Williamson GJ, Bindoff NL, Bowman DM. Climate–vegetation–fire interactions and feedbacks: trivial detail or major barrier to projecting the future of the Earth system?. *Wiley Interdisciplinary Reviews: Climate Change*. 2016 Nov; 7(6):910–31.
16. Battlori E, Ackerly DD, Moritz MA. A minimal model of fire-vegetation feedbacks and disturbance stochasticity generates alternative stable states in grassland–shrubland–woodland systems. *Environmental Research Letters*. 2015 Mar 19; 10(3):034018.
17. Kitzberger T, Perry GL, Paritsis J, Gowda JH, Tepley AJ, Holz A, Veblen TT. Fire–vegetation feedbacks and alternative states: common mechanisms of temperate forest vulnerability to fire in southern South America and New Zealand. *New Zealand Journal of Botany*. 2016 Apr 2; 54(2):247–72.
18. Hantson S, Arneth A, Harrison SP, Kelley DI, Prentice IC, Rabin SS, Archibald S, Mouillot F, Arnold SR, Artaxo P, Bachelet D. The status and challenge of global fire modelling. *Biogeosciences*. 2016; 13(11):3359–75.
19. Sullivan AL. Wildland surface fire spread modelling, 1990–2007. 1: Physical and quasi-physical models. *International Journal of Wildland Fire*. 2009 Jul 20; 18(4):349–68.
20. Sullivan AL. Wildland surface fire spread modelling, 1990–2007. 2: Empirical and quasi-empirical models. *International Journal of Wildland Fire*. 2009 Jul 20; 18(4):369–86.
21. Sullivan AL. Wildland surface fire spread modelling, 1990–2007. 3: Simulation and mathematical analogue models. *International Journal of Wildland Fire*. 2009 Jul 20; 18(4):387–403.
22. Rabin SS, Melton JR, Lasslop G, Bachelet D, Forrest M, Hantson S, Li F, Mangeon S, Yue C, Arora VK, Hickler T. The Fire Modeling Intercomparison Project (FireMIP), phase 1: Experimental and analytical protocols. *Geoscientific Model Development*. 2017 Mar 17; 20:1175–97.
23. Keane RE, McKenzie D, Falk DA, Smithwick EA, Miller C, Kellogg LK. Representing climate, disturbance, and vegetation interactions in landscape models. *Ecological Modelling*. 2015 Aug 10; 309:33–47.
24. Norby RJ, Zak DR. Ecological lessons from free-air CO₂ enrichment (FACE) experiments. *Annual review of ecology, evolution, and systematics*. 2011 Dec 1; 42:181–203.
25. Way DA, Oren R, Kroner Y. The space-time continuum: the effects of elevated CO₂ and temperature on trees and the importance of scaling. *Plant, cell & environment*. 2015 Jun; 38(6):991–1007.
26. Hendrey GR, Ellsworth DS, Lewin KF, Nagy J. A free-air enrichment system for exposing tall forest vegetation to elevated atmospheric CO₂. *Global Change Biology*. 1999 Mar; 5(3):293–309.
27. Ainsworth EA, Long SP. What have we learned from 15 years of free-air CO₂ enrichment (FACE)? A meta-analytic review of the responses of photosynthesis, canopy properties and plant production to rising CO₂. *New Phytologist*. 2005 Feb; 165(2):351–72. <https://doi.org/10.1111/j.1469-8137.2004.01224.x> PMID: 15720649
28. Brodrigg TJ, McAdam SA, Jordan GJ, Feild TS. Evolution of stomatal responsiveness to CO₂ and optimization of water-use efficiency among land plants. *New Phytologist*. 2009 Aug 1; 183(3):839–47. <https://doi.org/10.1111/j.1469-8137.2009.02844.x> PMID: 19402882

29. Van Der Sleen P, Groenendijk P, Vlam M, Anten NP, Boom A, Bongers F, Pons TL, Terburg G, Zuidema PA. No growth stimulation of tropical trees by 150 years of CO₂ fertilization but water-use efficiency increased. *Nature geoscience*. 2015 Jan; 8(1):24.
30. Omernik JM, Griffith GE. Ecoregions of the conterminous United States: evolution of a hierarchical spatial framework. *Environmental management*. 2014 Dec 1; 54(6):1249–66. <https://doi.org/10.1007/s00267-014-0364-1> PMID: 25223620
31. Bachelet D, Ferschweiler K, Sheehan TJ, Sleeter BM, Zhu Z. Projected carbon stocks in the conterminous USA with land use and variable fire regimes. *Global change biology*. 2015 Dec; 21(12):4548–60. <https://doi.org/10.1111/gcb.13048> PMID: 26207729
32. Van Wagner CE, Forest P. Development and structure of the canadian forest fireweather index system. InCan. For. Serv., Forestry Tech. Rep 1987.
33. Canadian Forestry Service. Tables for the Canadian Forest Fire Weather Index System. Environment Canada, Canadian Forestry Service; 1984.
34. Daly C, Halbleib M, Smith JI, Gibson WP, Doggett MK, Taylor GH, Curtis J, Pasteris PP. Physiographically sensitive mapping of climatological temperature and precipitation across the conterminous United States. *International Journal of Climatology: a Journal of the Royal Meteorological Society*. 2008 Dec; 28(15):2031–64.
35. Abatzoglou JT, Brown TJ. A comparison of statistical downscaling methods suited for wildfire applications. *International Journal of Climatology*. 2012 Apr 1; 32(5):772–80.
36. Eidenshink J, Schwind B, Brewer K, Zhu ZL, Quayle B, Howard S. A project for monitoring trends in burn severity. *Fire ecology*. 2007 Jun 1; 3(1):3–21.
37. Hudiburg T, Law B, Turner DP, Campbell J, Donato D, Duane M. Carbon dynamics of Oregon and Northern California forests and potential land-based carbon storage. *Ecological applications*. 2009 Jan 1; 19(1):163–80. PMID: 19323181
38. Turner DP, Ritts WD, Kennedy RE, Gray AN, Yang Z. Regional carbon cycle responses to 25 years of variation in climate and disturbance in the US Pacific Northwest. *Regional environmental change*. 2016 Dec 1; 16(8):2345–55.
39. Law BE, Turner D, Campbell J, Sun OJ, Van Tuyl S, Ritts WD, Cohen WB. Disturbance and climate effects on carbon stocks and fluxes across Western Oregon USA. *Global Change Biology*. 2004 Sep; 10(9):1429–44.
40. Peterman W, Bachelet D, Ferschweiler K, Sheehan T. Soil depth affects simulated carbon and water in the MC2 dynamic global vegetation model. *Ecological modelling*. 2014 Dec 24; 294:84–93.
41. Pew KL, Larsen CP. GIS analysis of spatial and temporal patterns of human-caused wildfires in the temperate rain forest of Vancouver Island, Canada. *Forest ecology and management*. 2001 Jan 1; 140(1):1–8.
42. Syphard AD, Radeloff VC, Keeley JE, Hawbaker TJ, Clayton MK, Stewart SI, Hammer RB. Human influence on California fire regimes. *Ecological applications*. 2007 Jul; 17(5):1388–402. PMID: 17708216
43. Rorig ML, Ferguson SA. Characteristics of lightning and wildland fire ignition in the Pacific Northwest. *Journal of Applied Meteorology*. 1999 Nov; 38(11):1565–75.
44. Dorado FC, Pérez JR, Menéndez JL, Taboada MF. Modelling the probability of lightning-induced forest fire occurrence in the province of León (NW Spain). *Forest Systems*. 2011(1):95–107.
45. Rienstra JT, Yeiter MA, Teensma PD. Preliminary reconstruction and analysis of change in forest stand age classes of the Oregon Coast Range from 1850 to 1940. United States Department of the Interior Bureau of Land Management Technical Note T/N OR-9. Portland Oregon. 1991, Oct.
46. Law BE, Hudiburg TW, Berner LT, Kent JJ, Buotte PC, Harmon ME. Land use strategies to mitigate climate change in carbon dense temperate forests. *Proceedings of the National Academy of Sciences*. 2018 Mar 16:201720064.
47. Dale VH. The relationship between land-use change and climate change. *Ecological applications*. 1997 Aug; 7(3):753–69.
48. Dale VH, Joyce LA, McNulty S, Neilson RP, Ayres MP, Flannigan MD, Hanson PJ, Irland LC, Lugo AE, Peterson CJ, Simberloff D. Climate change and forest disturbances: climate change can affect forests by altering the frequency, intensity, duration, and timing of fire, drought, introduced species, insect and pathogen outbreaks, hurricanes, windstorms, ice storms, or landslides. *AIBS Bulletin*. 2001 Sep; 51(9):723–34.
49. Bentz BJ, Régnière J, Fettig CJ, Hansen EM, Hayes JL, Hicke JA, Kelsey RG, Negrón JF, Seybold SJ. Climate change and bark beetles of the western United States and Canada: direct and indirect effects. *BioScience*. 2010 Sep 1; 60(8):602–13.

50. Gonzalez P, Neilson RP, Lenihan JM, Drapek RJ. Global patterns in the vulnerability of ecosystems to vegetation shifts due to climate change. *Global Ecology and Biogeography*. 2010 Nov; 19(6):755–68.
51. Westerling AL. Increasing western US forest wildfire activity: sensitivity to changes in the timing of spring. *Phil. Trans. R. Soc. B*. 2016 Jun 5; 371(1696):20150178. <https://doi.org/10.1098/rstb.2015.0178> PMID: 27216510
52. Turner DP, Ritts WD, Kennedy RE, Gray AN, Yang Z. Effects of harvest, fire, and pest/pathogen disturbances on the West Cascades ecoregion carbon balance. *Carbon balance and management*. 2015 Dec 1; 10(1):12.
53. Tedim F, Leone V, Amraoui M, Bouillon C, Coughlan MR, Delogu GM, Fernandes PM, Ferreira C, McCaffrey S, McGee TK, Parente J. Defining extreme wildfire events: difficulties, challenges, and impacts. *Fire*. 2018 Feb 25; 1(1):9.
54. Barbero R, Abatzoglou JT, Larkin NK, Kolden CA, Stocks B. Climate change presents increased potential for very large fires in the contiguous United States. *International Journal of Wildland Fire*. 2015 Nov 5; 24(7):892–9.
55. Dennison PE, Brewer SC, Arnold JD, Moritz MA. Large wildfire trends in the western United States, 1984–2011. *Geophysical Research Letters*. 2014 Apr 28; 41(8):2928–33.
56. Parente J, Pereira MG, Amraoui M, Fischer EM. Heat waves in Portugal: Current regime, changes in future climate and impacts on extreme wildfires. *Science of the Total Environment*. 2018 Aug 1; 631:534–49. <https://doi.org/10.1016/j.scitotenv.2018.03.044> PMID: 29529441
57. Senf C, Seidl R. Natural disturbances are spatially diverse but temporally synchronized across temperate forest landscapes in Europe. *Global change biology*. 2018 Mar; 24(3):1201–11. <https://doi.org/10.1111/gcb.13897> PMID: 28881439
58. Sommerfeld A, Senf C, Buma B, D'Amato AW, Després T, Díaz-Hormazábal I, Fraver S, Frelich LE, Gutiérrez ÁG, Hart SJ, Harvey BJ. Patterns and drivers of recent disturbances across the temperate forest biome. *Nature communications*. 2018 Oct 19; 9(1):4355. <https://doi.org/10.1038/s41467-018-06788-9> PMID: 30341309
59. Thomas D, Butry D, Gilbert S, Webb D, Fung J. The Costs and Losses of Wildfires. 2017 Nov 2.
60. Spies TA, White E, Ager A, Kline JD, Bolte JP, Platt EK, Olsen KA, Pabst RJ, Barros AM, Bailey JD, Charnley S. Using an agent-based model to examine forest management outcomes in a fire-prone landscape in Oregon, USA. *Ecology and Society*. 2017 Mar 1; 22(1).
61. Preisler HK, Hicke JA, Ager AA, Hayes JL. Climate and weather influences on spatial temporal patterns of mountain pine beetle populations in Washington and Oregon. *Ecology*. 2012 Nov; 93(11):2421–34. PMID: 23236913
62. Enright NJ, Fontaine JB, Bowman DM, Bradstock RA, Williams RJ. Interval squeeze: altered fire regimes and demographic responses interact to threaten woody species persistence as climate changes. *Frontiers in Ecology and the Environment*. 2015 Jun; 13(5):265–72.
63. Malcolm JR, Markham A, Neilson RP, Garaci M. Estimated migration rates under scenarios of global climate change. *Journal of Biogeography*. 2002 Jul; 29(7):835–49.
64. Gruenwald NJ, Goss EM, Press CM. *Phytophthora ramorum*: a pathogen with a remarkably wide host range causing sudden oak death on oaks and ramorum blight on woody ornamentals. *Molecular Plant Pathology*. 2008 Nov; 9(6):729–40. <https://doi.org/10.1111/j.1364-3703.2008.00500.x> PMID: 19019002
65. Neary DG, Ice GG, Jackson CR. Linkages between forest soils and water quality and quantity. *Forest ecology and management*. 2009 Oct 30; 258(10):2269–81.